CFD-Matlab
Thermal Comfort Study

Design of a coupling system to exchange data between CFD programmes and a human thermal comfort model

Eva Bernat Fuentes (evabe235)

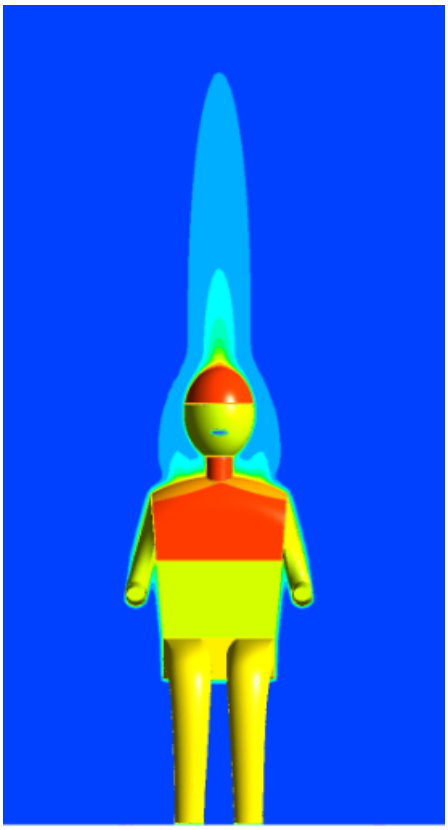

LINKÖPINGS UNIVERSITET

Linköping University | Department of Management and Engineering
Master's thesis, 30 credits | Master in Aeronautical Engineering
Spring 2020 | LIU-IEI-TEK-A–20/03892—SE

Linköping University | Department of Management and Engineering
Master's thesis, 30 credits | Master in Aeronautical Engineering
Spring 2020 | LIU-IEI-TEK-A–20/03892—SE

CFD-Matlab Thermal Comfort Study

Design of a coupling system to exchange data between CFD programmes and a human thermal comfort model

---

Eva Bernat Fuentes (evabe235)

Academic supervisor: Jörg Schminder (LiU)
Industrial supervisors: Roland Gårdhagen (LiU)
Examiner: Matts Karlsson (LiU)

LINKÖPINGS UNIVERSITET

Linköping universitet
SE-581 83 Linköping, Sverige
013-28 10 00, www.liu.se

Abstract

The general trend of increasing heat loads in modern passenger aircraft cabins e.g. caused by in-flight entertainment or novel energy sources, induces a rising demand for efficient yet comfortable ventilation systems. Therefore, the typical design and dimensioning criteria of conventional Aircraft Cabin Ventilation system concepts need to be verified to avoid problems concerning the thermal sensation and comfort of the passengers. Fanger's Predicted Mean Vote-method is traditionally used for estimating thermal sensation and comfort. The PMV method does not take into account the human thermoregulatory system, therefore it progressively over-estimates the mean perceived warmth of warmer environments and the coolness of cooler environments. Aircraft Cabin CFD models existing in the industry tend to make use of constant temperature boundary condition to define a human being. The compromise on accuracy that this fact generates, brings the doubt about how making more realistic simulations. Human thermoregulatory models represent the human body from a thermokinetic point of view and they have been used for modelling the thermoregulation system. Their tissue heat transfer, thermal sensation and thermal comfort calculation has been successfully validated under various steady-state and transient indoor environment boundary conditions comparing the simulation results to measurements made with real human beings.

From an existing Matlab model of a human being (approximated with 9 layers and 15 body parts) provided by Espuna [1], the main goal of this work is to connect it to the three-dimensional cabin model in ANSYS Fluent developed by Raina et. al. [2]. From it, local environmental conditions around a human body and the response of the human body to these conditions could be obtained, such as transient temperature changes at the skin. These last ones will be fed back to the CFD model to enable the effect that the body has on the local environment. This two-way data transfer has been thought to be important when modeling spaces with low air velocities according to Cropper [3], due to the impact that human body has on the local environment. The model regards an aircraft cabin. This simulation will have the goal of optimizing the thermal comfort for the passengers. The ventilation conditions tested will be Displacement Ventilation (DV) and a transient Thermal Comfort Model will be applied at a local and global level for each human.

Acknowledgements

This master thesis was performed at Linköping University at the Department of Engineering in the spring of 2020. With a deep sense of gratitude I would like to acknowledge all those who contributed significantly towards the successful completion of this project.

Especially, my supervisors Jörg Schminder and Roland Gårdhagen, who contributed in the day-to-day development issues of this project. Their dynamism, vision, sincerity and motivation have deeply inspired me. Emphasizing Jörg's empathy and great sense of humour. I would also like to thank Hossein Nadali Najafabadi for his valuable input on developing the room model and vast knowledge on computational heat transfer subject.

Besides my advisors, I would like to thank the examiner Matts Karlsson for the keen interest to complete this thesis successfully, as well as his encouragement, insightful comments, and hard questions. Last but not the least I would like to thank my family and friends for their constant source of inspiration and support. Thanks to Carmen, for her constant support at personal fulfillment. Also to Leny, Matt, Caro, Paz, Alba, Mauri, Carla, Ricard and Alex who have been my family in Linköping.

Finally, I would like to dedicate this thesis to my grandfather Miguel, for being my inspiration and the first light of life - my engineer father and my raiser.

Nomenclature

Abbreviations and Acronyms

Abbreviation	Meaning
LiU	Linköping University
CFD	Computational fluid dynamics
CAD	Computer aided design
CPU	Central processing unit
HTRM	Human Thermo-Regulatory Model
HVAC	Heating, Ventilation and Air Cooling
UDF	User Defined Function
PMV	Predicted Mean Vote
STB	Simplified Thermoregulatory Bio-Heat Equation

Latin Symbols

Symbol	Description	Units
act	activity level	$[met]$
f_{cl}	clothing area factor	
h_c	convective heat transfer coefficient	$\left[W \cdot m^{-2} \cdot K^{-1}\right]$
h_r	radiative heat transfer coefficient	$\left[W \cdot m^{-2} \cdot K^{-1}\right]$
i_{cl}	moisture permeability index from the skin to the skin surface	
I_{cl}	clothing insulation	$[clo]$
q_{conv}	convective heat transfer flux	$\left[W \cdot m^{-2}\right]$
$q_{rad_{long}}$	long-wave radiative heat transfer flux	$\left[W \cdot m^{-2}\right]$
$q_{rad_{sh}}$	short-wave radiative heat transfer flux	$\left[W \cdot m^{-2}\right]$
q_{evap}	evaporative heat transfer flux	$\left[W \cdot m^{-2}\right]$
t_o	operational temperature	$[^oC]$
RH	relative humidity	

Greek Symbols

Symbol	Description	Units
ϵ	Difference in the mean skin temperature between two data exchanges	$[^oC]$
β	Thermal expansion coefficient	$[1/K]$

Contents

1 Introduction

Nowadays, industry is highly interested in developing simulation systems that allow us to observe the human response in a given product during the design process, that's why digital twins are created. Both the automotive and aeronautical industry are examples that invest in the development of human thermoregulation models to predict the resulting degree of comfort or discomfort a person experiences. Major aircraft manufacturers, such as Boeing and Airbus, have been improving the comfort level of their cabins in order to meet this demand. As a consequence of it, a major scope is then focused in providing effective design tools to improve building thermal performance, improve occupant comfort and reduce energy consumption. One of these tools could be an integrative simulation which includes an aircraft cabin and a digital twin of a human.

The general trend of increasing heat loads in modern passenger aircraft cabins e.g. caused by in-flight entertainment or novel energy sources, induces a rising demand for efficient yet comfortable ventilation systems. Although the industry is working on a reversal of this general trend by identification and application of more sustainable solutions for cabin related heat loads, novel ventilation concepts can support the effort to reduce the energy consumption of the environmental control system and may be accompanied by other benefits like improved thermal passenger comfort or reduced cabin weight.

To approach this, computational fluid dynamics (CFD) is a computer modelling technique that is able to predict in considerable detail the complex patterns of airflow and air temperature distribution. It has been used successfully to predict the likely ventilation performance of many advanced naturally ventilated buildings (e.g. Short and Cook 2005 [4]). A CFD model provides temperatures and velocities of airflow around a human body, whereas that the thermoregulatory model (HTRM) predicts the response of human body to detailed local environmental conditions. The thermoregulatory model attemps to be a digital twin of a human body, which is a digital replica of a living or non-living physical entity, in terms of heat transfer for this case. Numerical models are advantageous as it is extremely difficult to predict human responses for non-uniform conditions with high resolution by experiments.

In design practice, simple shaped blocks are often used to represent human occupants in CFD models and derive empirically based thermal comfort parameters such as predicted mean vote (PMV) and predicted percentage of dissatisfed (PPD). PMV results show that the environment is comfortable or not. This PMV model has become the internationally accepted model for describing the predicted mean thermal comfort of occupants in indoor environments.The answer to "why we would need integrated CFD and human models" seems simple: on the human side, we want more resolution and accuracy in the calculation of heat transfer at the boundary; on the environment side, we want the environmental quality (e.g. thermal comfort) to be evaluated by human response rather than thermometer reading.

The new integrated simulation system, which couples the standalone CFD aircraft cabin simulation with the thermoregulatory model, will support engineers in the detailed stages of the aircraft development process and in the development and optimization of ECS and HVAC systems.

From an existing Matlab model of a human being (approximated with 9 layers and 15 body parts) provided by Espuna [1], the main goal of this work is to connect it to the three-dimensional cabin model on ANSYS Fluent developed by Raina et. al. [2]. From it, local environmental conditions around a human body and the response of the human body to these conditions could be obtained, such as transient temperature changes at the skin. These last ones will be fed back to the CFD model to enable the effect that the body has on the local environment. This two-way data transfer has been thought to be important when modeling spaces with low air velocities according to Cropper [3], due to the impact that human body has on the local environment.

1.1 Literature study

The computational thermal manikin, based on the coupled simulation of convection, radiation, moisture transport, and human thermal physiological model, was first defined and proposed by Murakami et al. (1997) [5]. A simplified body shape was used without modeling body parts such as legs and hands separately. Tanabe et. at. (2002) integrated a 65-node human thermoregulatory model with a 3D model of a male body in CFD which incorporated radiation heat transfer.

Al-Mogbel (2003) [6] used a simplified shape to represent a human body in CFD in Ansys Fluent and coupled this with a two-node thermal regulatory model (Gagge et. al. 1986). Finally, a CFD code was obtained to map regions of Thermal Comfort, using 2 different thermal comfort indices. The model represented a standing human in a naturally ventilated room. Its aim was determining the total (sensible+latent) heat transfer of the human body, and to predict thermal comfort zone in the room.

More recently, Cropper et al. (2010) [3] have investigated and validated with numerical and experimental work, the same topic modelling a standing human subject in a naturally ventilated environment in the context of a non-domestic building. The Institute of Energy and Sustainable Development (IESD) developed a new version of Fiala creating IESD-Fiala. Using IESD-Fiala for the thermoregulatory model, Ansys CFX as the CFD software and CFX Expression Language (CEL) functions as the communication interface between both softwares. The reason for embedding IESD-Fiala model in CFD is motivated since in transient studies the CFD software must have the possibility to update boundary conditions for each time step during solver execution cycle. However, differences between the simulations and experimental results were not published. Both naked [3] and clothed [7] manikins were tested and heat transfer coefficients for individual body parts were reported.

Fiala (2004) [8] used the method of exchanging data between two models for cars industry; consisting of network sockets and data files. It was used in the INKA car simulator which used a simple approach using locally stored files. INKA is state-of-the-art simulation software that provides comprehensive predictions of the prevailing, time-varying thermal environment in automobiles. From it, we can obtain the knowledge of how to connect the human model with the car. In order to get realistic simulations for the liked car - occupant system, thermal interactions occurring between the passengers and the indoor environment were modelled. These include e.g. the warming of the occupied zone by the realease of bodily heat and changes in the water vapour content of the air due to respiration and moisture evaporation from the body surface, as well as the dynamic heat loss from body parts in contact with car surfaces. To capture these effects it was imperative that the new simulation system enabled a bi-directional, dynamic data exchange between the models. To achieve it, the simulation deploys as two parallel processes that are coupled via a communication interface with controls the exchange of the simulated data for each time step of a simulation run. It will be important that there is a matching between every geometry part, (i.e. every single part of the body in which it is splitted), of the CFD model mesh and the thermoregulatory model mesh.

Dixit et. al. (2015) [9], worked with a seated human model in a ventilated room and used Ansys Fluent with the help of a User Defined Function (UDF, writtten in C script) to assign the temperatures of the skin interface from the thermoregulatory model. With UDFs the user can define a customized boundary profile (like the temperature of the skin, obtained from the HTRM) which varies as a function of time and/or space (for instance, every part of the body can be defined with a different temperature). As it can be found in the ANSYS Fluent UDF manual [10], to define the temperature at a boundary, the "Define Profile" macro is needed, with which the designer can customize the boundary profile as written previously. The thermoregulatory model used is based on Fanger's model (which accounts for passive response) but with adding the Simplified Thermoregulatory Bio-Heat Equation (STB) (which accounts for active response). That will fix the fact that Fanger's model by itself is uncapable to account active thermoregulatory activities such as vasomotion, sweating and shivering etc. which are inherent from transient simulations. Since the STB equation can be solved within the CFD tool itself, it also avoids the need of a separate standalone model for human body thermoregulation simulation. The inner human was solved inside Fluent, in which surfaces, the equation of the simplified thermoregulatory bio-heat equation is applied as a Boundary Condition in a UDF file. It contains two boundary conditions: the skin boundary condition and the core boundary condition.

Martinho et. al. (2012) [11] developed a study of a human manikin in a standard 3D-room comparing it with experimental results. The aim was evaluating possible CFD errors and determining the importance of considering an appropriate turbulence model (k- ω SST vs. k-ϵ) and the contribution of radiation effects. It was concluded that approximately 40% of heat transfer in human body was due to radiation (vs. convection), and that SST was a better model to predict heat fluxes near wall.

Yang (2008) [12] described specifically in practical words, how to adapt Fiala code calculations in order to interface IESD-Fiala model with ANSYS CFX. Some of heat transfer components from Fiala were simplified. They neglected conductive and short wave radiation (irradiation) heat transfer effects because of being insignificant. They focused on heat transfer due to convection, long wave radiation and evaporation. Likewise Cropper [3] did, but added, however, short wave radiation. Local effects may be of interest if, for example, incident short-wave radiation is locally absorbed at parts of the body while the air condition supplies a stream of air to some of the other parts.

Yang (2017) [13] revealed the importance of using a multinode thermoregulatory model, such as Fiala is. First researchers, like Murakami (1999) [14], used a two-node thermal model in the coupling system. When a two-node thermal model is applied, the thermal responses of individual body segments cannot be predicted. Actually, human beings are always exposed to non-uniform environments and human thermoregulatory highly depends on local heat transfer characteristics. Therefore, it is inappropiate to evaluate thermal physiological responses at whole body level and a multi-node thermal model is required.

Gao (2005) [15] critically reviewed issues in CFD simulation using a numerical thermal manikin, such as turbulence model selection, grid generation and boundary conditions. The low Reynolds number k-ϵ model performs better in the prediction of heat loss from human body while the standard k- model and RNG k-ϵ model are sufficient if the emphasis is on airflow field.

De Dear (1996) [16] provided an experimental study of convective and radiative heat transfer coefficients for individual human body segments for a human female nude body, which is until today, the most accepted study. Nevertheless, this study splitted the body in big areas, like only 8 body parts.

Sorensen et Voigt (2003) [17] developed a CFD model of flow and heat transfer around a seated naked human body, providing details such as a plot graph of velocities above the human head, which eases verification of new CFD models, such as the one that is developed at the present work. Even though, Sorensen's model was only CFD based, with a constant temperature in the skin of the human as a boundary condition. It was not connected to a HTRM.

1.1.1 Objective

The aim of this master thesis consists of developing an integrated coupled simulation system for predicting both the dynamic, non-uniform environmental conditions in an aircraft cabin (CFD) and the human physiological and perceptual reponses under these complex circumstances. This simulation will have the goal of improving the thermal comfort for the passengers. For that, different ventilation conditions will be compared in order to see which one offers the best thermal comfort.

To split this big task, there are sub-objetives:

- To create the software connection with a simple domain in Ansys and Matlab as an example *(AAS Toolbox)*.
- To implement a 3D-room CFD case to analyze software connection with a single human manikin. Design a 3D-room CAD and couple it with the manikin geometry.
- To setup a CFD model running a RANS Turbulence model to simulate natural ventilation.
- To couple thermoregulatory model in Matlab with the CFD model in ANSYS by means of the first connection done *(AAS Toolbox)* to analyse heat transfer trends.
- To design the coupled case for the aircraft cabin. To split the mesh of the human manikin for having the 15 parts required by the HTRM.
- To run the RANS Turbulence model that is already provided by Raina et. al. [2] with the coupling of *AAS Toolbox*.
- To analyze the different ventilation systems and study their performance on thermal comfort by evaluating velocity and temperature profiles measured at locations close to the occupants in the cabin.

Limitations

The present thesis doesn't mean to focus on developing a new case of a CFD study but studying heat transfer effects between humans and the environment. This means that the following features are not going to be studied:

- CFD of the aircraft cabin study provided by Raina et. al.[2] is going to be treated as a special case of application and the CFD model is not going to be improved.
- HRTM model is quite elementary and is not either the focus of improvement.

Moreover, concerning the used model there are also some inherent limitations. Firstly, the detailed 3-D models of human in the CFD environment represented the naked body, which is unlike the case in every day environment. It is perceivable that the shape and posture of the model may have a significant impact on the local convective and radiant heat transfer coefficients. Models of clothed body should be studies to quantify such impact. Secondly, evaporation at the skin surface is a complex process, which is connected with moisture transportation due to convection. In the studies where evaporation was considered, empirical methods rather than CFD were used.

2 Theory

2.1 Thermoregulatory Model

The thermoregulatory Model that has been used was developed by Espuna [1] in 2017 for Matlab software. This HTRM model is based on Fiala's model (1998) which has been adapted to pressure changes in altitude for aeronautical applications and also with some modifications from Tanabe (2002) for clothing [1]. This Fiala model uses environmental parameters, such as the temperature at the skin surface, to predict the response of the human thermoregulatory system to these external stimuli over a period of time.

Fiala thermal comfort model consists of two interacting systems: the controlling active system and the controlled passive system.

2.1.1 Active system

The active system is in charge of regulating body temperature to mantain a stable value of temperature in the body core. The thermoregulatory system activates four kinds of response to regulate the body temperature: vasodilatation, perspiration, vasoconstriction and shivering. In hot conditions, vasodilatation and sweating are activated, to excrete moisture at the skin which evaporates producing the cooling of the body. However, in cold conditions, vasoconstriction is activated with shivering, an increase of the metabolic internal heat generation by contraction of muscles.

The active system was developed by means of statistical regression using measured data from several experiments ranging from steady state to transient cold stress, cold, warm and hot stress conditions, and different activity levels, from low to high exercise.

2.1.2 Passive system

The passive system is a multi-segmental, multi-layered representation of discretized human body and information about geometrical body properties.

The body is represented as 15 spherical and cylindrical elements built of annular concentric tissue layers with the appropriate thermo-physical properties and physiological functions. In each of the 15 so called elements or body parts, there is a maximum of 9 tissue layers, which would correspond into a discretization of 135 nodes in total amount. Each tissue can be made of one of the following elements: brain, lung, viscera, skin, bone, muscle. (See Figure 1).

The sizes and composition of the 15 body parts, are contained in the Matlab script "$HTRM_{basic}.m$" which enables easily different body characteristics to be modeled.

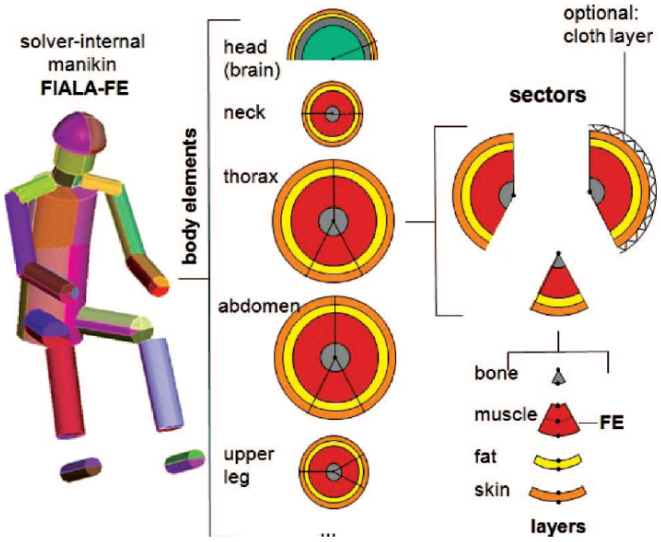

Figure 1: Fiala's approach to the human discretization. 15 body parts and segmentation. Extracted from [18]

Heat transfer equations in the model account for convection and radiation (long and short-wave) with the environment; internal heat production and blood heat exchange; and clothing insulation from the environment.

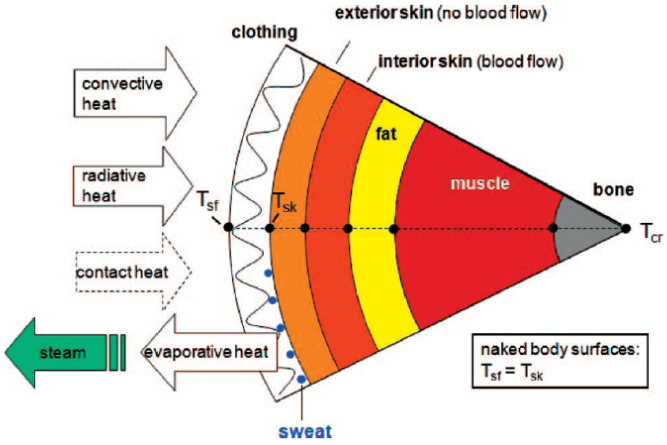

Figure 2: Sector-wise discretization of the concentric layer model and treatment of heat exchange with the ambient. Extracted from [18]

Clothing might be treated as additional layer that differs from the original Fiala model as shown in Figure 2. Via blood circulation, metabolic heat is transported to different elements and by radial conduction to the body surface where it is transferred to the environment by convection, radiation, evaporation and, if applicable, respiration and conduction, on the basis of the bioheat equation proposed by Pennes (1948), Equation 1.

$$k(\frac{\partial^2 T}{\partial r^2} + \frac{\omega}{r} + \frac{\partial T}{\partial r}\Big) + q_m + \rho_{bl} w_{bl} c_{bl}(T_{bl_a} - T) = \rho c \frac{\partial T}{\partial t} \quad (1)$$

The differential equation models the heat transfer in human tissues with a cylindrical model, where k represents the tissue conductivity ($W \cdot m^{-1} \cdot K^{-1}$), T the tissue temperature (°K), r the radius (m) and ω is a dimensionless geometric factor (ω = 1 for cylinders, ω = 2 for spheres). q_m denotes the metabolic heat production (W/m^3), which consists of a basal value plus the local autonomic thermoregulation while shivering. The last therm on the left-hand side of Equation 1 represents blood perfusion, where ρ_{bl} stands for the density (kg/m^3), w_{bl} for perfusion rate (s^{-1}), c_{bl} for the heat capacity ($J \cdot kg^{-1} \cdot K^{-1}$) and $T_{bl,a}$ for the arterial blood temperature (C). For the blood circulation, a central blood pool is assumed by modelling an exchange within the arterial and venous vascular system and by neglecting the heat storage within the vascular system. The metabolism q_m and blood perfusion rate w_{bl} are thereby influence by the active control system. Only radial heat conduction is considered as the surface areas of the interfaces between two sectors are insignificant compared with the surface areas of the sectors themselves. With respect to the skin moisture evaporation, a partial differential equation is used to describe the moisture accumulation and sweat production as predicted by the active system. For the respirative exchange, which again depends on the metabolism, it is distinguished between dry and latent heat exchange, which is distributed along the pulmonary tract.[18]

According to Fiala's work [19], the present model represents an average male weighting 73.5 kg, with 14 % of body fat, a skin surface area of 1.86 m^2, a cardiac output of 4.9 L/min, and a basal metabolic rate of 87.1 W.

2.1.3 Limitations

The model is simplified in such a way that it presenst the following limitations [1]:

- Only radial heat transfer is considered through the cylinders.
- Heat variations in the longitudinal direction are neglected.
- Every part of the body is represented as a cylinder or a sphere.

2.2 CFD

In this section, several basic CFD concepts that will be used in the Method section are explained to ease the general understanding for the reader.

2.2.1 Meshing

Meshing strategy is focused on three fundamental aspects: accuracy, efficiency and ease of generation.

Accuracy involves to have an adequate quality mesh in order to pre achieve convergence and a viable result. Efficiency means that cell count and element type are adequate to the available time to solve and isn't big enough to outgrow the actual Random Access Memory (RAM). And finally, ease of generation which means that setting up is going to take a reasonable amount of time. The goal is to find best compromise between accuracy, efficiency and ease of generation.

Fluent Meshing is similar to Workbench Meshing but it's more powerful though. It has more element types and more flexible customizations. Specially, it is considered to be an optimal tool to develop high quality meshes for complex geometries in an easier and faster way.

Inside Fluent Meshing there are several element types that can be created, each for their own benefit. Prisms are used to capture the boundary layer, the quality can be reduced around complex surfaces so it's important to make sure that the geometry is repaired. A tech grid is used to resolve areas of high complexity with good resolution. However, it can take quite a time to solve. The next best thing for that is the polyhedral grid that it combines a couple of tet elements to make a polyhedral element. The benefit of that is that it can actually reduce cell count and CPU time at the expense of requiring extra RAM. In case a hexahedral grid is possible to be due, it has the advantages versus the poly that it's got a smaller grid so it should take quicker to actually run. When a hexahedral grid is not possible to be due and a polyhedral would require high computational capacities, an intermediate solution such as a polyhex mesh could be optimal.

A useful tool to check near wall behaviour where viscous effects dominates is Y+. Y+ corresponds to a dimensionless distance normal to the wall which is measured in order to check that the flow in the boundary layer develops correctly, which is given by the Equation 2.2.1:

$$y^+ = \frac{\rho y u_\tau}{\mu} \tag{2}$$

where ρ is the density, μ is dinamic viscosity, y distance normal to the wall in global units and u some tangencial velocity scale.

2.2.2 Boussinesq Model

The Boussinesq model is a simplification that can be used for many natural-convection flows in order to achieve a faster convergence. Otherwise, when natural convection is dominant in the flow, the problem is required to be set up with fluid density as a function of temperature, which is computationally expensive. By removing density (ρ) from Navier-Stokes equations, the memory requirement is reduced as well as the degree of non-linearity. Boussinesq model treats density as a constant value in all solved equations [20], except for the buoyancy term in the momentum equation, expressed in Equation 3:

$$(\rho - \rho_0) \cdot g \approx -\rho_0 \beta (T - T_0) \cdot g \tag{3}$$

Where ρ_0 is the (constant) density of the flow, T_0 is the operating temperature, and β is the thermal expansion coefficient. Equation 3 is obtained by using the Boussinesq approximation to eliminate ρ (the density at each point of the domain) from the buoyancy term. Equation 3 is obtained by using the Boussinesq approximation defined in Equation 4.

$$\rho = \rho_0 \cdot (\beta (T - T_0)) \tag{4}$$

This approximation is accurate as long as changes in actual density are small; specifically, according to the Manual [20], the Boussinesq approximation is valid when Equation 5 is fulfilled.

$$\beta \cdot (T - T_0) \ll 1 \tag{5}$$

In practical words, errors of 1% at room temperature are obtained if Equation 6 is fulfilled. In the case of room ventilation with a human in the room, the maximum difference of temperatures would correspond to the values: T = 34^oC (on the head of the human) and $T_0 = 21^oC$ which is the room temperature, this would lead to a difference of 13°C, where Boussinesq model is valid.

$$\Delta T = \begin{cases} T - T_0 < 2^oC & Water \\ \\ T - T_0 < 15^oC & Air \end{cases} \tag{6}$$

2.3 Zhang's thermal sensation and thermal comfort model

Zhang (2010) ([21], [22]) developed a thermal sensation model to predict local and overall sensations, and local and overall comfort in non-uniform transient thermal environments. The model predicts human subjective responses to the environment from thermophysiological measurements or predictions. From body HTRM parameters such as the local skin and core temperature, the local thermal sensation can be obtained. The overall thermal sensation and comfort are calculated as a function of the local skin temperatures and the core temperature, and their change over time. These parameters are calculated for each of the body parts. Zhang's model seems to be more applicable than the usually used PMV model, which rests on steady state heat transfer theory and this state never precisely occurs in daily life. Moreover, de Dear and Brague (1998) found that the PMV overestimates the subjective warmth sensations of people in warm naturally ventilated buildings. [16]

Zhang (2010) proposes that the local thermal sensation S_{local}, (see Eq. 7), is a logistic function of local skin temperature, presented as the difference between the local skin temperature and its set point:

$$S_{local} = 4\left(\frac{2}{1+e^{-C1\cdot(t_{skin,loc}-t_{skin,loc,set})-K1[(t_{skin,loc}-\overline{t_{skin}})-(t_{skin,loc,set}-\overline{t_{set}})]}}\right), \\ +C2_i\frac{dt_{skin,loc}}{dt} + C3_i\frac{dt_{core}}{dt} \tag{7}$$

where $t_{skin,loc}$ is the local skin temperature, $t_{skin,loc,set}$ is the local skin set point temperature, $\overline{t_{skin}}$ is the mean whole-body skin temperature and $\overline{t_{set}}$ is the mean whole-body skin set point temperature. K1, C1, C2 and C3 are specific regression coeffficients for every body part. When the derivatives of skin and core temperatures (second and third term on the right-hand side of the equation) are zero, the model predicts thermal sensation in a steady state condition. In the method section, it is explained how the set point temperatures were calculated. These set points are the temperatures at which there is a neutral thermal reaction of the body.

The logistic function shows a linear relationship between the skin temperature and thermal sensation when the skin temperature is near its set point, but levels off when the skin temperature differs from the set point. When the local skin temperature differs from the local skin temperature set point, the sensation reaches the sensation scale limits between +4 and -4, ranging from very hot to very cold, (see Table 4).

Table 4: Thermal Sensation index (Zhang 2010).

Index	Thermal sensation
4	very hot
3	hot
2	warm
1	slightly warm
0	neutral
-1	slightly cool
-2	cool
-3	cold
-4	very cold

The overall thermal sensation S_0 is a weighted average of all the local sensations:

$$S_0 = \frac{\sum(weight_i S_{local,i})}{\sum(weight_i)} \tag{8}$$

where S_{local} represents the local sensation for segment i, and $weight_i$ is the weighting factor for that segment. The weighting factors are based on measurement results from 3 different types of conditions: uniform environments, step change transient between 2 different environments, and heating/cooling of local body parts under cool/warm ambient environments.

Local Comfort by Zhang is a piecewise linear function of local and overall thermal sensations calculated in Equation 9. It depends of regression coefficients for every

body part (C31, C32, C6, C71, C72, C8 and n), and the overall thermal sensation, S_0. S_0^- is the overall thermal sensation (if $S_0 < 0$) and S_0^+ is the warm overall thermal sensation (if $S_0 > 0$).

$$LocalComfort = \left[\frac{\frac{-4-(C6+C71|S_0^-|+C72|S_0^+|)}{|(-4+C31|S_0^-|+C32|S_0^+|+C8)|^n} - \frac{-4-(C6+C71|S_0^-|+C72|S_0^+|)}{|(4+C31|S_0^-|+C32|S_0^+|+C8)|^n}}{e^{25(S_l+C31|S_0^-|+C32|S_0^+|+C8)} + 1} + \frac{-4-(C6+C71|S_0^-|+C72|S_0^+|)}{|(4+C31|S_0^-|+C32|S_0^+|+C8)|^n} \right] \cdot [(S_1+C31|S_O^-|+C32|S_O^+|+C8)^n] + (C6+C71|S_0^-|+C72|S_O^+|) \quad (9)$$

Likewise, a thermal comfort index was implemented, having limits between +4 and -4, ranging from very comfortable to very uncomfortable (see Table 5). The overall comfort is the average of the two minimum local comfort votes.

Table 5: Thermal Comfort index (Zhang 2010)

Index	Thermal comfort
4	very comfortable
2	comfortable
+0	just comfortable
-0	just uncomfortable
-2	uncomfortable
-4	very uncomfortable

3 Method

In this section, the full methodology is going to be thoroughly explained in a chronological order. First, how the first connection between programmes had been done. Secondly, what were the modifications to the thermoregulatory model to be able to interface it with a CFD programme. Inner modifications to the thermoregulatory code were required to develop a system of inputs and outputs. Thirdly, how was the coupling algorithm developed, in order to give response at the question to when and how data exchange should take place. Finally, the construction of the CFD cases in Ansys Fluent and their validation.

3.1 Working in a simple connection between Fluent and Matlab

There are a couple of ways to connect Matlab results with Fluent: one is between shared files, which involves the use of Fluent journal and Gambit, and the other one is scripting Fluent directly from Matlab with the "AAS" Server Mode.

Figure 3 shows the two available models that have to be connected so that each one of them can be improved. The interface that is provided by Ansys to connect Fluent with Matlab, permits to obtain the same output in Matlab as if you were writting the commands in Ansys console. It also demonstrates how to execute Fluent commands from a Matlab session. The following subsections show the options that have been found so far to be able to connect the two softwares.

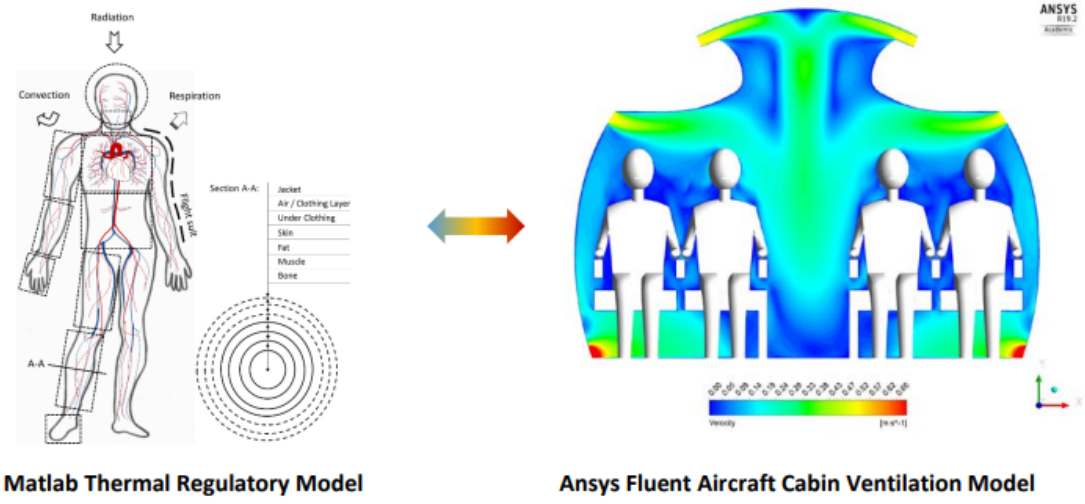

Figure 3: The subjects of the study.

3.1.1 MATLAB "AAS" Toolbox

Matlab "AAS" is a toolbox available for Matlab in which it is used As A Server (AAS) for Ansys programs. This seems to be the best option to connect ANSYS and MATLAB, if the user does not have high programming skills and overall knowledge of programming languages, among which, especially programs like FORTRAN, JAVA, C++. The toolbox can be downloaded from the ANSYS customer service portal and easily installed on MATLAB. It is also pretty straight forward to make a first connection with ANSYS. This is the tool that was finally used. It allows to transfer parameter variables easily between two softwares. The manual "ANSYS as a Server Example: MATLAB setup" [23] has been used to install Ansys Fluent server in the personal computer. The manual "ANSYS Fluent as a Server User's Guide" [24] can be consulted in order to understand Matlab commands which produce the actions in Fluent and control the whole simulation.

Since the functions of writing and reading parameters from Fluent that were explained in the manual [24] (page 49), were not working, these had to be implemented for the present work.

3.1.2 Journal Files

Journal files also seems to be a good option to be implemented to connect MATLAB and ANSYS to realize a dynamic connection between them. In fact, they are used to automate a series of commands instead of inputting them step by step in the command line [20]. They can also be used to create a record of the input to a program session for later reference. The only problem is that they do not seem to be as straight forward to use like the MATLAB "AAS" Toolbox and at the same time they do not seem to be as powerful as UDFs. However, there could be a chance to use the "AAS" Toolbox together with journal files. Then the three tools found to connect the two models might in the end be used together to create the best possible connection.

3.1.3 Back up Option: Profiles definition Within Ansys

As a backup option, the profiles definition option under the "boundary conditions" feature within ANSYS could be utilized. With this, the user can read and/or write profiles defined usually as .csv or .prof files. So, for instance, an array or a matrix obtained from the MATLAB model can be saved with these formats and, later on, uploaded manually to ANSYS to be assigned as a boundary condition to the passengers inside the Fluent model.

3.2 Modifications to the HTRM

The thermoregulatory model provided was fully working in a standalone mode. Nonetheless, it was required to be modified to create input parameters for a CFD program, and that means, to substitute the external physics ocurring out of the skin, such as environmental convection and radiation. The original thermoregulatory model considered that air flow was approaching towards the human body with a constant velocity and at an average temperature. Moreover, extra modifications had to be done such as the calculation of clothing temperature, which was missing in the implementation of the code.

3.2.1 Clothing insulation

The HTRM provided by Espuña [1] treats clothing insulation as Tanabe (2002) [25]. The cloth isn't modeled as an extra layer of the discretized body, but rather as a "thermal resistance". It means, there isn't specifically a node for the cloth layer, but the heat transfer coefficient from the environment to the skin, is reduced by an empirical equation in order to account for insulation effects (see Equation 10).

$$h_t = \frac{1}{0.155 \cdot I_{cl} + \frac{1}{(h_c+h_r)f_{cl}}} \tag{10}$$

Where h_t is the equivalent total heat transfer coefficient, h_c is the convective heat transfer coefficient, h_r is the radiative heat transfer coefficient, I_{cl} is the moisture permeability index from the skin to the skin surface, and f_{cl} is the clothing area factor.

For the present work, a naked person has been tested in order to be able to compare results with Cropper [7] and available experimental results. Nevertheless, in case in future works this coupling system investigation could further developed, it has been modified also for having clothing option. The I_{cl} that was set as a uniform value, has been modified to the I_{cl} values for the Kansas State Uniform (KSU) + summer clothing that has been widely used in the research and specifically in the works of Cropper (2009,2010) [3], Yang [13], Zhang et. Yang [12]. The aim is to ease the possible comparison in case a clothed body might be simulated.

Moreover, the calculation of the temperature of the cloth, T_{cl} has been added, as shows Equation 11. It will make possible to state the temperature of the surface in the CFD case when a clothed body is treated.

$$T_{cl} = (T_{sk} - T_{air}) \cdot \frac{\frac{1}{h_c+h_r}}{\frac{1}{h_t}} + T_{air} \tag{11}$$

Where T_{cl} is the cloth temperature, T_{sk} is the temperature of the skin and T_{air} is the operative room temperature of the sorrounding air.

3.3 Interface connection between CFD Fluent and Fiala

To interface Fiala model with the commercial package, some modifications to the Fiala model are necessary. The aim is to replace the empirical calculations of environmental heat transfer in Fiala model with Fluent simulation results. Fiala model considers total heat transfer between human body and the environment as a sum of 7 components including: conduction (q_{cond}), convection (q_{conv}), long ($q_{rad_{long}}$), short wave radiation ($q_{rad_{sh}}$), and evaporation at the body surface (q_{evap}), as well as respiratory convective and evaporative heat losses (q_{resp}) [12], as shown in Equation 12.

$$q_{sk} = q_{cond} + q_{conv} - q_{rad_{sh}} + q_{rad_{long}} + q_{resp} - q_{evap} \tag{12}$$

For each sector of the passive system heat balances are established as boundary conditions at the surface, as shown in Figure 4.

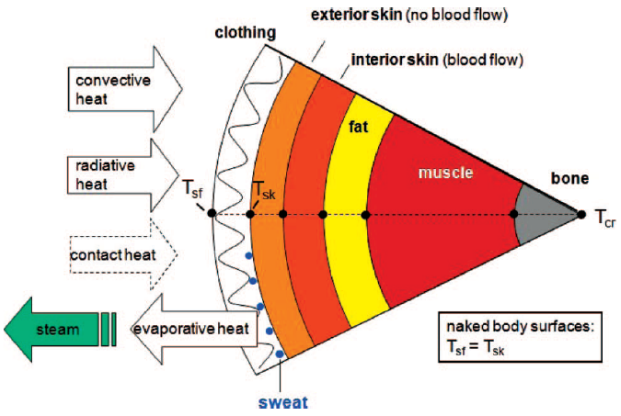

Figure 4: Sector-wise discretization of the concentric layer model and treatment of heat exchange with the ambient. Extracted from [18]

The net skin heat loss, q_{sk} (W/m^2) of a sector exposed to ambient air is equivalent to the sum of individual components of the environmental heat loss. Conduction is neglected because it is insignificant for this example. Respiratory heat losses are computed using the existing empirical equations in the Fiala model, except the condition of inhaled air (domain average air temperature and moisture content) could be obtained from Fluent. We focus on the heat transfer due to convection (q_{conv}), long wave radiation ($q_{rad_{long}}$), short-wave radiation ($q_{rad_{sh}}$) and evaporation ((q_{evap})). This results in Equation 13.

$$q_{sk} = q_{conv} - q_{rad_{sh}} + q_{rad_{long}} - q_{evap} \tag{13}$$

In an attempt to improve this model because all heat transfer components are calculated from empirical correlations. The idea is to provide some of heat transfer flux components that can be calculated directly from CFD. In line with this logic,

convection and long wave radiation at skin surface is going to be calculated by CFD. Meanwhile, Fiala model is going to calculate by empirical regressions all the rest components.

Then, CFD model is used to predict the convective heat flux (q_{conv}) and the long-wave radiative heat flux ($q_{rad_{long}}$)) at the skin surface. In response, Fiala model predicts the body surface temperature and evaporative heat loss flux resulting from evaporation of moisture at body surface (sweating) (q_{evap}) and short wave radiation (irradiation) ($q_{rad_{sh}}$). Cropper [3] has included the effect of short wave radiation for CFD prediction in the parameters exchange but in this study, it is not going to be taken into account.

3.3.1 Fiala standalone work-mode. Uncoupled

Figure 27 shows the calculation of total heat flux at the body surface (q_{sk}) in the Fiala model. The oval shapes identify variables/parameters, whereas the small circles represent equations/models. The mean ambient air temperature T_a, the air velocity v_a, and the surface temperature T_{surf} are used to calculate the convective heat transfer coefficient (h_{conv}) (see Fiala 1999 [19] for deeper details). Subsequenlty, convective heat flux (q_{conv}) is calculated. Similarly, the surface temperature T_{surf} and the mean radiant temperature of the room walls T_{env} are used to calculate the radiative heat flux (q_{rad}). The evaporative coefficient U_{evap} is calculated from h_{conv} by means of Lewis analogy. The mean ambient vapour pressure p_a and the skin vapor pressure p_{sk} are then used to calculate the evaporative heat loss E_{sk}. The surface heat flux q_{sk} is finally passed to the human mode for calculating internal thermal state of the body and its regulatory response (triggered by the active system), which consequently updates T_{surf} and p_{sk}. Then, p_{sk} is used to calculate the sweating mass fraction *dm-dt* of the skin. Any of both these parameters can be suitable to model moisture transfer to the environment if wished. When the manikin is modelled as naked, the temperature of the surface is the temperature of the skin. ($T_{surf} = T_{sk}$).

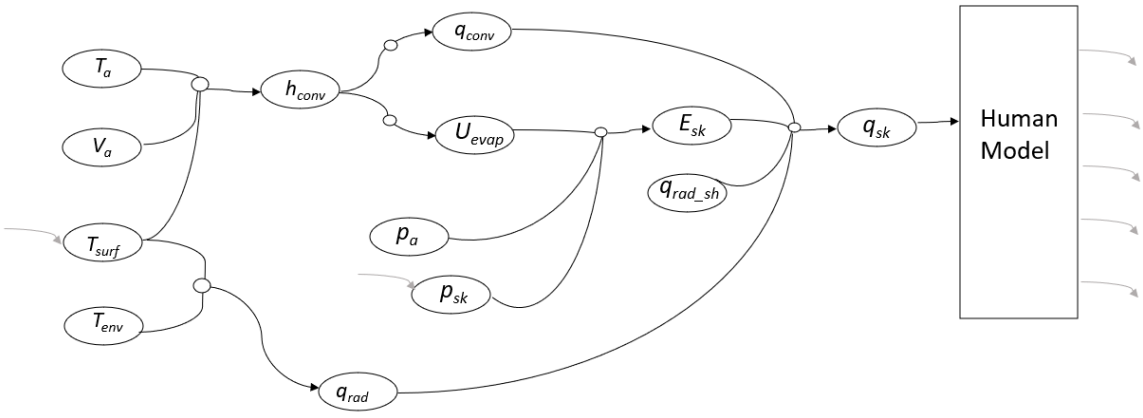

Figure 5: Flow chart calculation of heat transfer flux at skin surface by Fiala. If used in Standalone mode, without Coupling. Inspired by [12]

3.3.2 Fiala-CFD work-mode. Coupled

Figure 6 shows the flow chart of how the coupled system Fiala-CFD calculates the heat transfer flux at skin surface. Body surface temperature T_{surf} is imposed as a boundary condition of the CFD model, which solves the flow field as well as convective and radiant fluxes (q_{conv} and q_{rad}) [12] at manikin surface. Since h_{conv} is reversely calculated from q_{conv}, the evaporative heat loss is influenced also by the CFD simulation. If moisture transport is implemented, p_{sk} is also imposed as a boundary condition at CFD, and is introduced back at Fiala like the Relative Humidity of the room, RH. For validation simulations, moisture transfer is not implemented since it was not used in comparative studies.

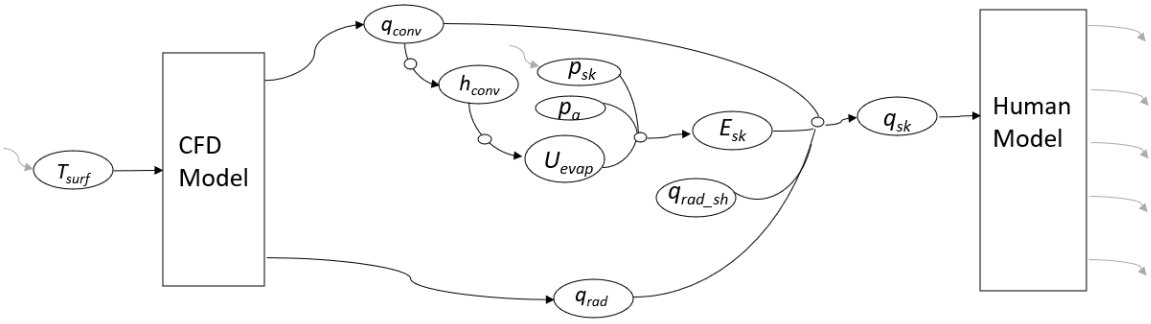

Figure 6: Flow chart calculation of heat transfer flux at skin surface by coupling CFD-Fiala. Environmental heat transfer calculation using CFD results. Inspired by [12]

3.3.3 Fiala model convergence

Fiala model is able to predict body's response to local environmental conditions that change over time, i.e. transient conditions. In this work, the coupled system models the interaction between local environment and the body under steady-state conditions. To achive that, Fiala model is run in a way that corresponds to the body being exposed to the same local conditions for a long period of time to make sure that the model reaches a steady state. Then, Fiala reaches convergence in every run.

3.3.4 The coupling algorithm

The coupling algorithm is designed in order to control all the coupled simulation by Matlab session and it is summarised in Figure 7. At the beginning of the coupled simulation, Fiala is run to provide an initial set of boundary conditions at the body surface. A first run takes an initial set of boundary conditions. Then, body surface temperatures for each of the 15 parts predicted by the initial simulation are written as Input Parameters and they are exported from Matlab to Fluent by means of "AAS" Toolbox function. The CFD solver is then run.

CFD solves a minimum number of iterations set and then, a new condition of stopping criteria is defined from Matlab Code. The new stopping criteria activates the Stop Condition for only the RMS residual values of continuity and momentum. The values of Stop Condition are set as 10^{-3} for continuity and 10^{-5} for momentum. When the latter residuals fall below the upper threshold and the minimum number of iterations between data exchanges has been completed, the convective heat flux and the radiative heat flux for each of the 15 body parts, are written as Output Parameters. These parameters are passed back to Matlab.

Fiala reads these Output parameters from the CFD calculation and provides new Inputs parameters again for the CFD simulation, building up a loop of data exchange. Data exchange is terminated if the difference in mean body surface temperature between consecutive data exchanges is less than a pre-set threshold. In this case it has been set to $\epsilon = 0.01$. The Fluent solver is then allowed to run without further data exchanges taking place until the desired level of CFD convergence is achieved. For this last step, the condition of stopping criteria is modified: all residuals for Stop Condition are activated and set to 10^{-5}. This value has been set as acceptable for convergence in most of engineering problems. Stabilization of monitor points can be also observed at Fluent session.

As the predictions from each model have an effect on the other, the overall predictions of the coupled system are the result of an iterative process of progressive refinement. The essence of this algorithm has been based and adapted to Matlab session from Cropper's algorithm [7]. The implemented code which englobes the coupling system and controls the coupled simulation has been attached and can be read in the Appendix section.

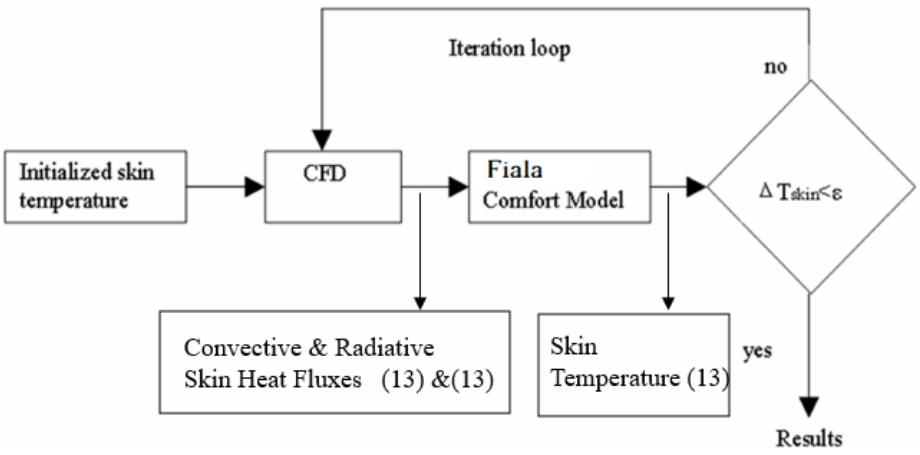

Figure 7: Coupling of CFD and Fiala model. Inspired by [26]

3.4 CFD Design. Human in a 3D simplified Room

A first simulation was carried out in a simple environment in order to simplify the boundary conditions which could lead to unstabilities in the coupling system. A 3D Room was decided to be performed to be also validated by similar research works. The commercial CFD code ANSYS Fluent, version 2019 R2, was used to model airflow and heat transfer. Steady-state simulations have been used to model the thermal conditions in an indoor environment with a human body as the only heat source.

3.4.1 Computer Aided Model (CAD)

The computational domain has been reproduced from the work done by Cropper [3], [7]. It consists of a box which dimensions of width and depth are 3 m (to omit horizontal aspect ratio effects) and a height of 2.5 m. The domain has four 0.25 m x 0.25 m ventilation openings at floor level and two 0.25 m x 0.25 m openings at ceiling level, defined as free openings. This configuration was motivated for having minimal effect on the thermal plume generated by the human located in the center of the room, the only driving force being the metabolic heat generated by the occupant.

The human geometry model is taken from the work done by Raina et. al. [2] and was conceived to represent a human passenger seated inside an aircraft.

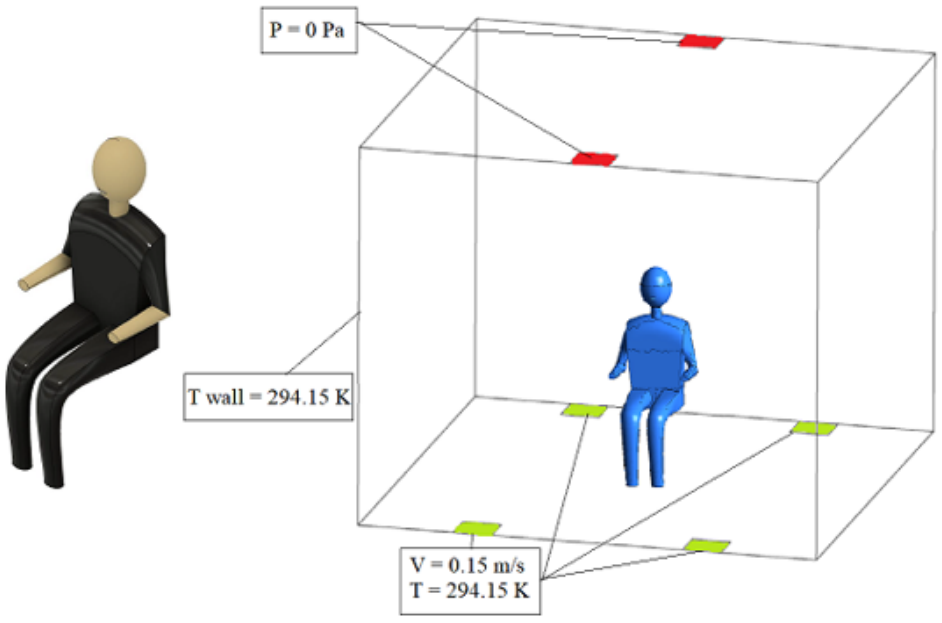

Figure 8: A computational thermal manikin in a naturally ventilated room with upper and lower openings. Inlets in green, outlets in red.

3.4.2 Model meshing

The mesh generation process was done in ANSYS Fluent meshing 2019 R2. The first step in meshing was to create a proper surface mesh. The surface mesh generated has a skewness of 0.55 which indicates a good mesh quality. Volume meshing is then generated with a hexahedral type with an orthogonal quality of 0.36 which also indicates a good enough quality of the mesh.

The manikin, which was subdivided into 13 body parts, had a total of 48,948 surface mesh elements. There were 10 prism layers are placed near manikin body and walls (see Figure 10). The computational domain is composed of approximately 1.1 million unstructured and structured elements. The body is covered by a body of influence to set a local mesh sizing of 2 mm.

The Enhanced Wall treatment method approach requires a very fine grid near wall region to capture the rapid variation of the variables. This imposes restrictions on the grid resolution in the near wall region, where it is desirable to have at least one node in the viscous sub layer ($y^+ < 11.1$). More specifically, it is recommended to use a value of $y^+ \sim 1$, as achieved in Figure 10. Vieser et. al. [27] presented a heat transfer validation test that studied grid sensitivity for a series of different parameters, and shows a very good agreement between experimental and numerical results for low values of y^+ (less than 3).

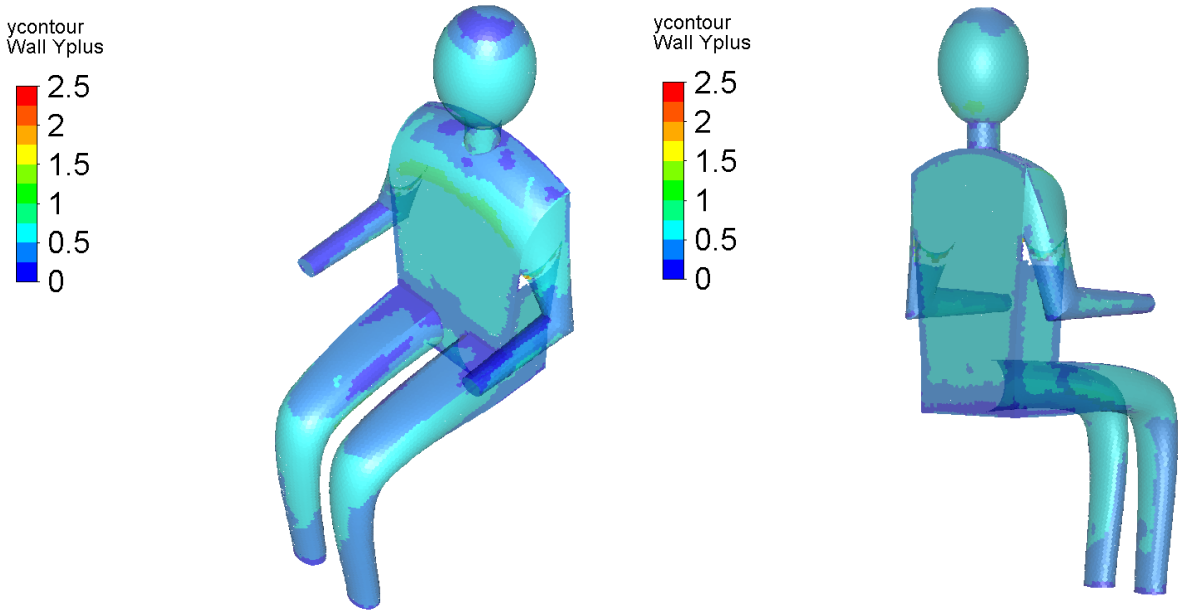

Figure 9: Y^+ **contours along human surface show that vast majority of areas have a value of less than 1.**

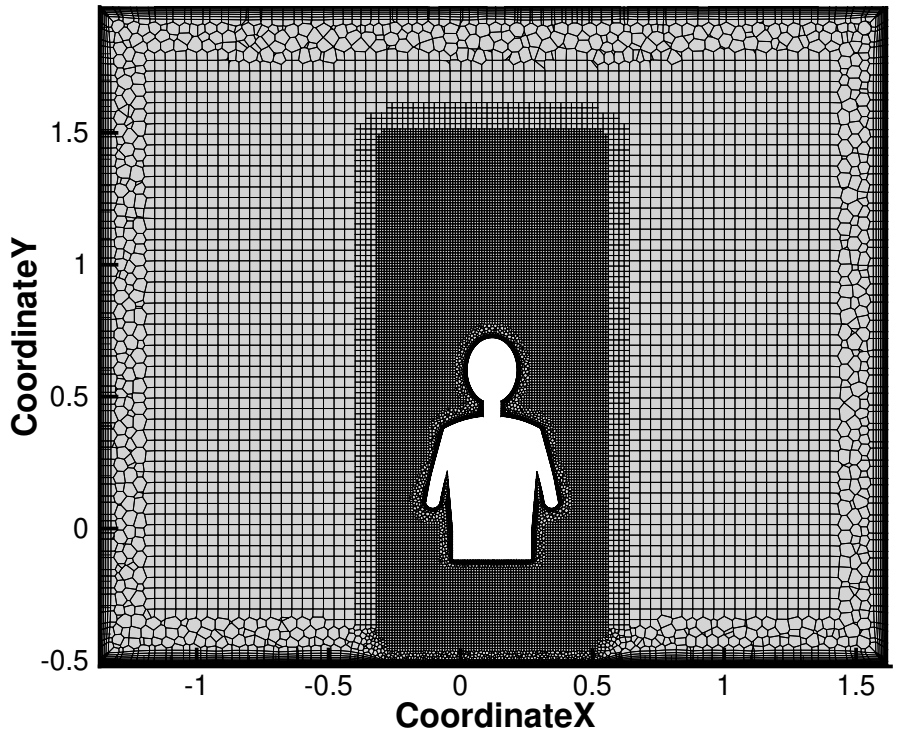

Figure 10: Simplified 3D room mesh using body sizing from body of influence and inflation layer of prisms cells created along human and room wall boundaries.

3.4.3 Physics to solve - Problem modelling

Due to the temperature difference between the human body and its surroundings, the airflow pattern close to the body can be a mixed convection flow or a natural convection flow which depends on whether the human body is placed in stagnant air or not. The importance of buoyancy forces in a mixed convection flow can be measured by the ratio of the Grashof and Reynolds numbers.

Rayleigh numbers less than 10^8 indicate a buoyancy induced laminar flow, with transition to turbulence occurring over the range of $10^8 < \text{Ra} < 10^{10}$. If it is assumed that the human body to be a cylinder with the height of 1.65m and radius of 0.15 m, the Reynolds number will exceed 2500 based on the equivalent diameter of 0.3 m as the characteristic length of a human body if the air velocity is more than 0.13 $m \cdot s^{-1}1$. When a human body is sitting in stagnant air, the Ra number will reach about 4.1 $\cdot 10^9$ at the head level, assuming the temperature difference is 9 ^oC. Therefore, in most cases the airflow around the human body is turbulent or is in the transition zone from laminar flow to turbulent flow. However, strictly speaking, the k-epsilon model is only applicable in the fully developed turbulent flow. It is difficult to reproduce the transition from laminar to turbulent with the k-epsilon model.

Furthermore, the k-epsilon model is not accurate enough for simulating the air flow field around a bluff body. Murakami et al. [5] used a contrived method on a k-epsilon model to simulate this transition flow by adding a slight turbulence generation term to the k-equation and epsilon-equation throughout the whole computational domain. Since there may be many typical flow elements, such as jet flow, buoyancy driven flow, laminar flow and potential flow, in the simulation of air flow in a ventilated room with a human body, no turbulence model which is now available can deal perfectly with this complex flow pattern. The k-epsilon model is the best choice for now among various turbulence models available in view of its simulation accuracy and computational expense. The low Reynolds number k-epsilon model performs better in the prediction of heat loss from human body while the standard k-epsilon model and RNG k-epsilon model are sufficient if the emphasis is on airflow field. In the presented case, there is mainly natural convection. Heat transfer occurs due to heat exchange by free and forced convection with ambient air. These imposed forced convective fluxes are to remove part of the metabolic heat produced by the human body.

Heat transfer modes that occur are convection and radiation. Martinho et. al. (2012) [11] developed a study of a human manikin in a standard 3D-room comparing it with experimental results. The aim was evaluating possible CFD errors and determining the contribution of radiation effects. It was concluded that approximately 40 % of heat transfer in human body was due to radiation (vs. convection). Hence, radiation is considered to be important to be modelled.

3.4.4 Solver setup

As the indoor temperature differences are relatively small, the Boussinesq approximation is used to model the effects of buoyancy. Buoyancy-driven flows inputs are set as "gravity on" and selecting boussinesq approximation. Boussinesq approximation is taken to model a variable density in air properties, as well as, thermal expansion coefficient is defined for air at room temperature. For the turbulence modelling, (RNG) k-ϵ was chosen due to its stability and precision of numerical results [15]. A discrete ordinates radiation model with rays was used to model radiant heat transfer. (Instead of Monte Carlo with 2 million histories, which Zhang [12] pointed out that gave similar results for a higher computational cost. The additional computational effort is relatively small because the DO model assumes that radiation is emited isotropically from each surface). In problems with localized sources of heat, the Discrete Ordinates model is probably the best suited for computing radiation for this case, although the DTRM, with a sufficiently large number of rays, is also acceptable [20]. Surfaces emissivity is treated as a constant having a value of 0.95 for body surface and 0.83 for surrounding surfaces. [16] [17].

Momentum had to be resolved with 1^{st} order upwind discretization scheme due to convergence problems with 2^{nd} order. The methods to configurate the software and get a solution step-by-step was consulted in the ANSYS MANUAL [20], section "How to Model Natural Convection and Buoyancy Driven Flows" . First, the calculations were run with a low Rayleigh (g = 0.098 m/s^2) and finally with full gravity.

The model settings are listed in Table 8.

Table 6: Solver Settings

Equations	Discretisation
p-v scheme	Coupled
Turbulence Model	RNG K-epsilon with EWT
Gradient	Least squares cell based
Pressure	Second order
Gradient	Least squares cell based
Momentum & Turbulence	1^{st} order upwind
Energy	2^{nd} order upwind
Discrete Ordinates	2^{nd} order upwind

3.4.5 Boundary Conditions

The boundary conditions that model the heat transfer problem are listed in Table 7.

Table 7: Boundary conditions applied

Region	Boundary Conditions	
Inlet	Velocity Inlet	0.15 m/s at 21°C
Outlet	Pressure Outlet	0 Pa
Wall	No Slip Wall	Fixed Temperature at 21 °C
Human	No Slip Wall	T_{sk} from Fiala or 31°C

3.4.6 Validation I: procedure and verification.

Two research studies have been used to validate the CFD model developed. First, Sorensen's simulation [17] has been tried to be reproduced in order to validate the CFD case in a standalone mode, without any connection of HTRM. It was required to validate flow and heat transfer behavior around a heat source with a human shape. As soon as the CFD simulation in standalone mode was proved to be validated, a second validation was required. Cropper's simulation with a naked person [7] was tried to be reproduced. This simulation already accounted for the validation of the connection between a HTRM and a CFD case.

For validation of the CFD-uncoupled case, the CFD has been set up with a boundary condition of constant temperature in the skin of 31°C, which is the same than Sorensen [17] has considered in his study. To further validate the CFD calculations, these are compared to experimental and numerical results. Experimental PIV measurements are provided in Figure 11, which shows the vertical velocity in a vertical plane x = - 0.12m (front view, approximately centred above the head). Numerical CFD results are also compared at whole body level in Figure 12. The agreement is satisfactory between Sorensen's experimental measurements [17] and this study's results.

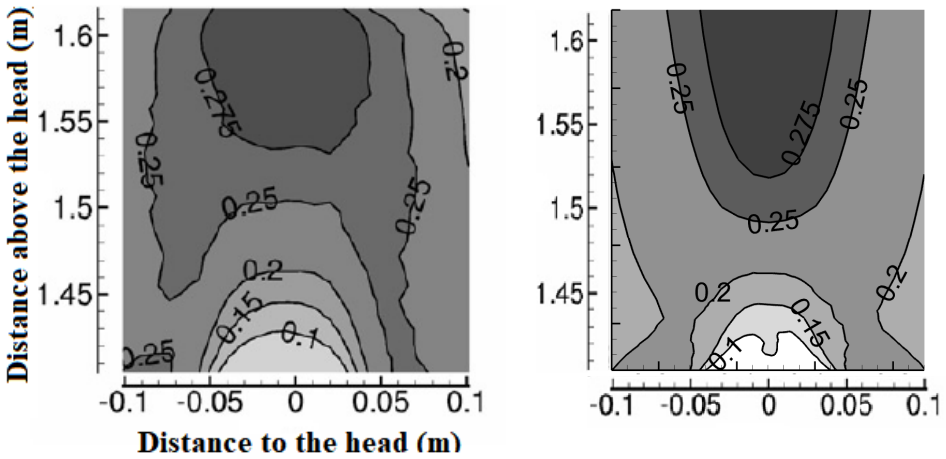

Figure 11: Validation of uncoupled case. Contours of vertical velocity (m/s), frontview in x = 0.12 (m) (centred near top of head). Left: measured*, right: calculated. ∗(Sorensen [17] experimental measurements. (T_{sk} = 31°C))

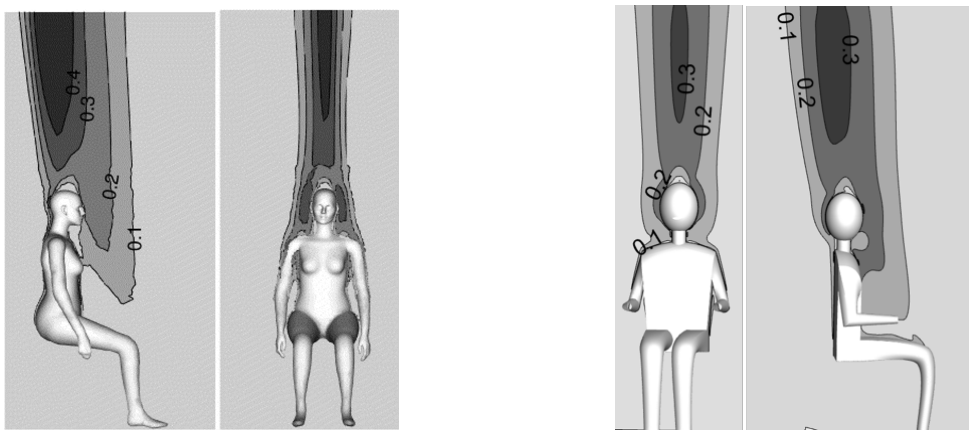

Figure 12: Validation of uncoupled case. Distributions of vertical velocity (m/s). Sideview in symmetry-plane (left) and frontview (right) (centred near top of head). Left: Sorensen*, right: calculated. ∗(Sorensen [17] CFD calculations. (T_{sk} = 31°C))

For the validation of the CFD-coupled case, the CFD has been set up with a boundary condition of Fiala skin temperature, which is the same than Cropper [7] has considered in his study. For it, Fiala has been configured in a similar way than Cropper had, that is a naked person. An activity level of 1.2 met has been used as it is the activity level a person would output if seated while reading. The temperature of the skin of Fiala has been imposed as a boundary condition to predict flow field.

3.4.7 Validation II: Heat transfer coefficients

Apart from a qualitative validation of flow contours, a quantitative validation is also required. The surface heat transfer coefficient is the heat flux (convective or radiative) divided by the difference between the local wall temperature and the near-wall air temperature. The heat transfer coefficient depicts the transfer of heat from the human to the room surrounding. The surface heat transfer coefficient is implemented from the available heat transfer variables under the wall fluxes category for post-processing in ANSYS Fluent. A User Defined Function has been implemented to obtain the convective heat transfer coefficient by dividing the convective heat flux by the temperature difference between the skin and the near-wall air temperature. The same procedure has been approached to obtain the radiative heat transfer coefficient. The near-wall air temperature that has been considered for this study is the room temperature (21^{o}C), because it is what all authors have taken for reference. The same temperature conditions are required to be able to establish a comparison.

As explained in Section Validation I, two cases are going to be compared: Case 0.A) Uncoupled Case, and Case 0.B) Coupled case. For each of them, radiative and convective heat transfer coefficients for each of 13 body parts are going to be compared with experimental [16], and other 2 CFD data [7] and [17]. Experimental coefficients were obtained by de Dear [16] (1997), in which a nude female manikin, whose skin temperature was maintained at a constant temperature, was placed in a test chamber. In this experiment, heat transfer coefficients were determined by measuring the energy required to maintain a constant surface temperature over 16 body regions. The combined heat loss, i.e. the sum of the convective and radiative components, was first determined. Selected areas of the manikin were then covered by a low Emissivity material and the experiment repeated in order to isolate the radiative component.

It is expected that Case 0.A) that is the uncoupled case, as shown in Figure 13, CFD Bernat (green line) (that is the case of this study) results are more similar to CFD Sorensen (pink line), since they both represent a naked seated human with a constant temperature of T=31^{o}C. Thicker lines were represented to highlight these two data sets. It is expected that Case 0.B) that is the coupled case, as shown in Figure 16, CFD Bernat (green line) results are more similar to CFD Cropper (yellow line), since they both represent a naked human with Fiala imposed body temperature. Thicker lines were represented to highlight these two data sets. Due to problems to compare heat transfer coefficients because authors defining different segmentation for body parts causing a possible mismatching, body plots have been attached when authors' data was found, in Figures 15b and 14b.

Contour plots of velocity and temperature distributions in the coupled simulation have also been attached in Figure 17 (bottom). It can be seen that the thermal plume develops over the height of the body and reaches a maximum speed of 0.32 m/s about 0.5 m above human head. The spatial air temperature distribution and surface temperature on the manikin body parts is also shown in Figure 17 (top), where it can be seen that the coupled system predicts a non-uniform surface temperature with the head and upper torso predicted to be at a higher temperature than the hands and legs.

Case 0. A) Uncoupled Case. CFD-only, T=31ºC

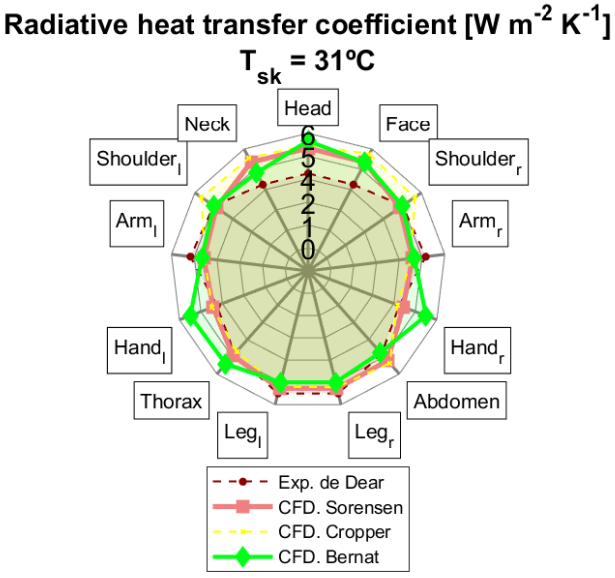

(a)

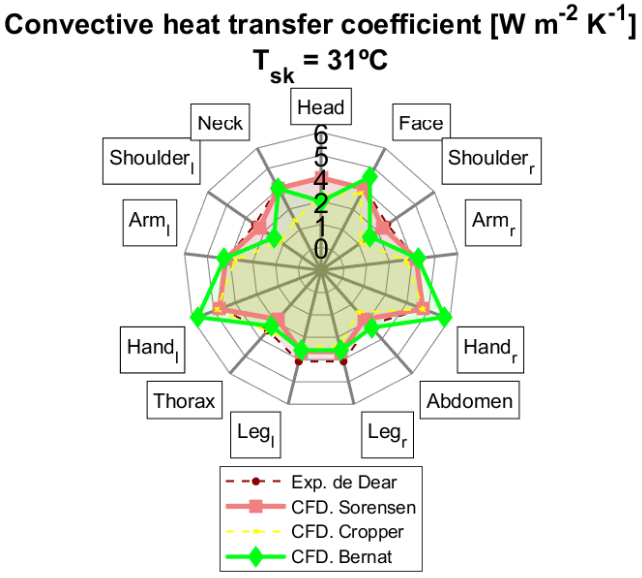

(b)

Figure 13: Radiative and convective heat transfer coefficients comparison and validation with a experimental setup by Dear[16], and 2 CFD cases: Cropper [3] and Sorensen [17]

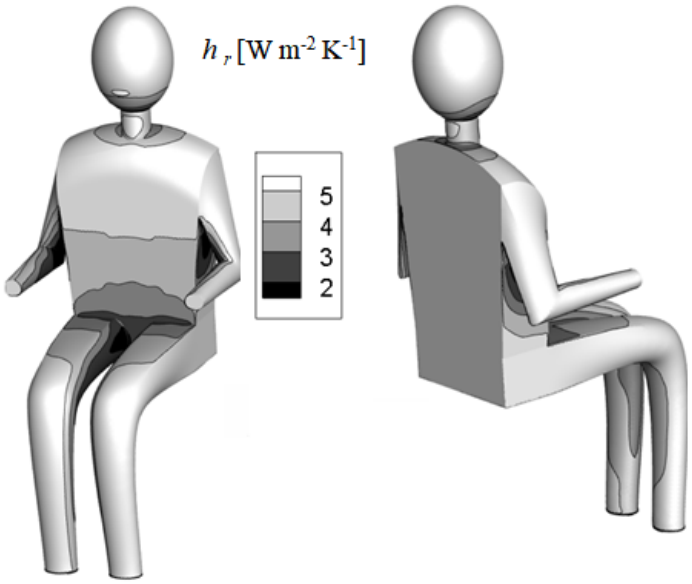

(a)

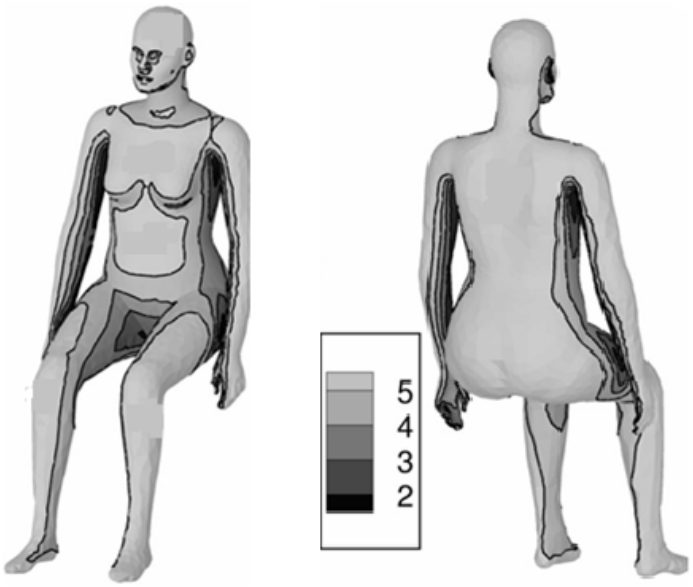

(b)

Figure 14: Radiative heat transfer coefficients comparison and validation with Sorensen [17]

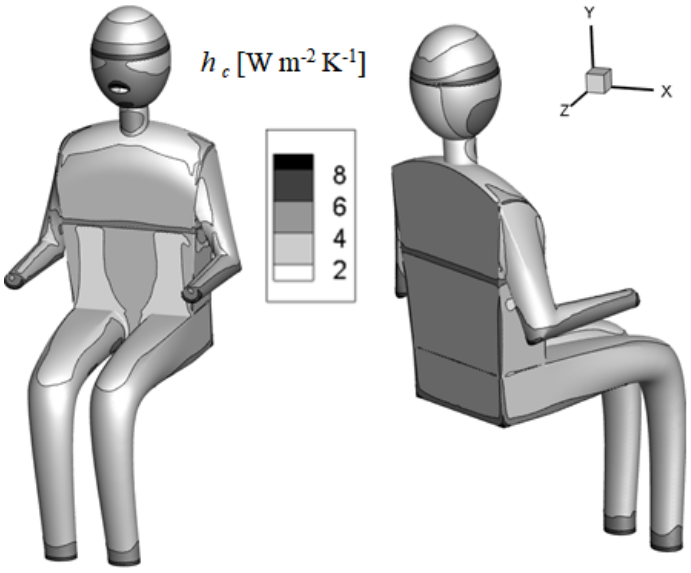

(a)

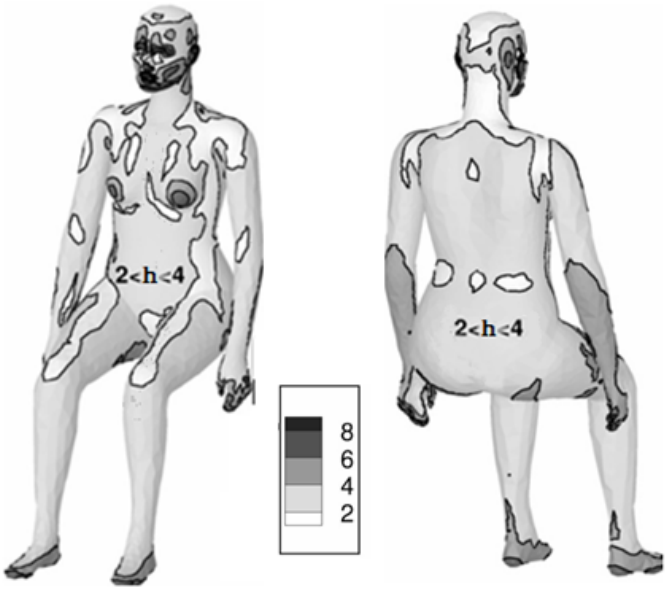

(b)

Figure 15: Radiative heat transfer coefficients comparison and validation with Sorensen [17]

Case 0. B) Coupled Case. CFD-HTRM, T= (Fiala) ºC

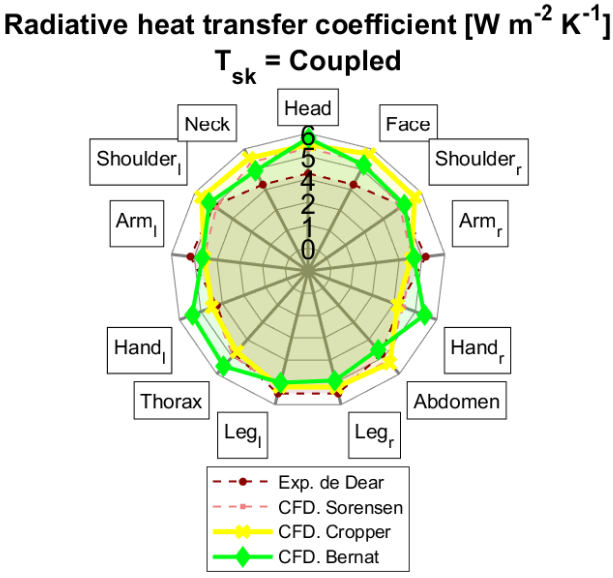

(a)

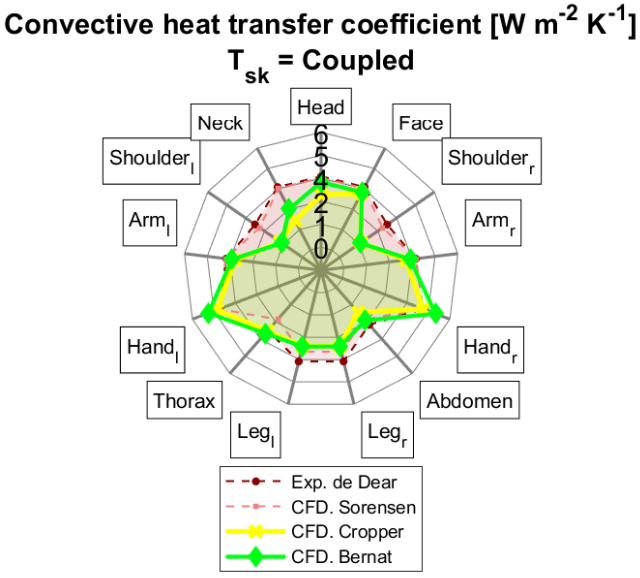

(b)

Figure 16: Radiative (a) and convective (b) heat transfer coefficients comparison and validation with a experimental setup by Dear[16], and 2 CFD cases: Cropper [3] and Sorensen [17]

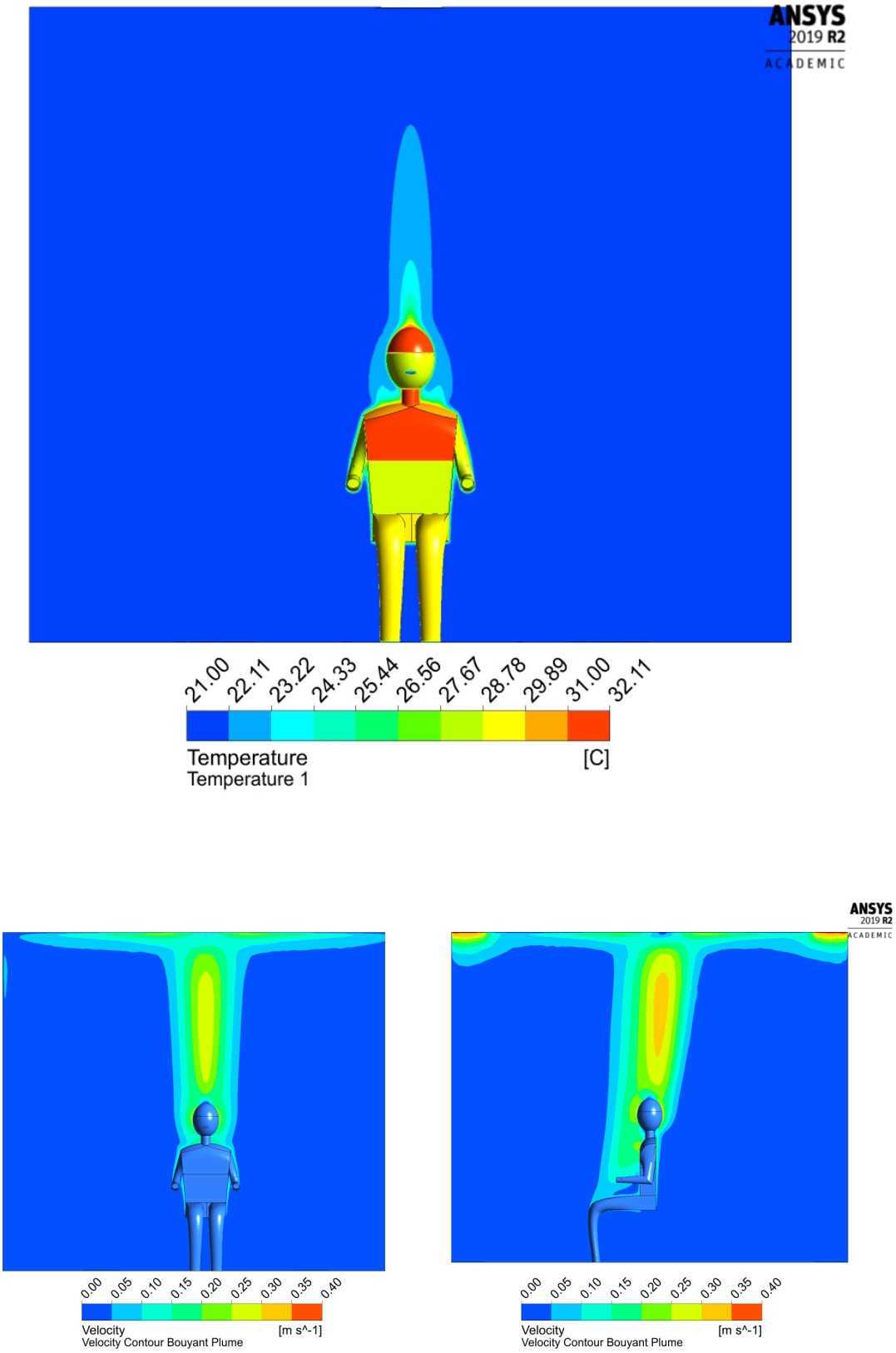

Figure 17: Temperature and velocity contour plots at sections crossing the center of the head of the manikin. Coupled simulation.

3.5 CFD Design Application. Human in the Cabin

The coupling system has been applied to an aircraft cabin model created by Raina et. al. [2]. It models a single aisle passenger cabin of a regional jet aircraft with human manikins as passengers. The inlets and outlets are modelled as strips by approximating ventilation inlet and outlet average nozzle areas from actual aircraft cabins. Although three different ventilation systems were studied, here displacement ventilation configuration (DV) will be coupled to the HTRM. Displacement ventilation is probably the best configuration to ensure convergence. That is because the flow is simply going upwards, without any big whirls that may cause instabilities.

3.5.1 CAD Model - Cabin

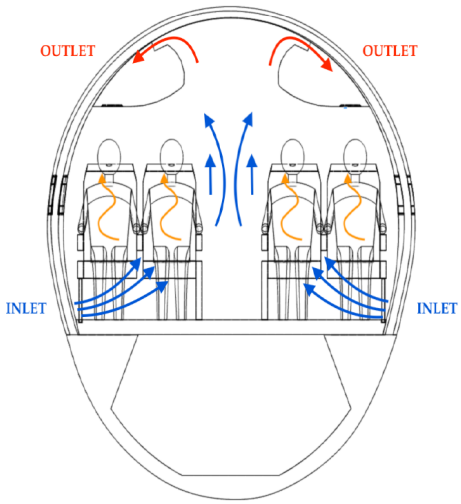

Figure 18: Displacement Ventilation configuration illustration. [blue arrows indicate fresh air realised from inlet diffuser, red arrows indicate outle for air exraction, yellow arrows depict thermal plumes arising from heat sources.

3.5.2 Human model

The human model that was used for this simulation was the same than used in Abishek et. al. [2], and that also was used in this thesis for the "Human in the 3D Room" part.

3.5.3 Model meshing

The mesh generation process was done in ANSYS Fluent meshing 2019 R2. The mesh could have been reused from Abishek et. al. [2] but since it required geometry modifications in the humans, a replica had to be done manually from scratch. A finer mesh is used closer to the human manikins, walls and overhead baggage bin because of the larger airflow and temperature gradients that are generated in their vicinity

(see Figure 19). The first step in meshing was to create a proper surface mesh. The surface mesh generated has a skewness of 0.65 which indicates a good mesh quality. Volume meshing is then generated with a polyhedral type with a maximum skewness of 0.92 and a minimum orthogonal quality of 0.28 which also indicates a good enough quality of the mesh.

The manikin was subdivided into 13 body parts. There were 10 prism layers are placed near manikin body and walls with a smooth transition. Yplus value of less than 1 is achieved with a growth ratio of 1.2. The computational domain is composed of approximately 7.7 million unstructured and structured elements. The bodies are covered by two bodies of influence (BOI) to set a local mesh sizing of 8 mm. Local face meshing is also employed on the walls.

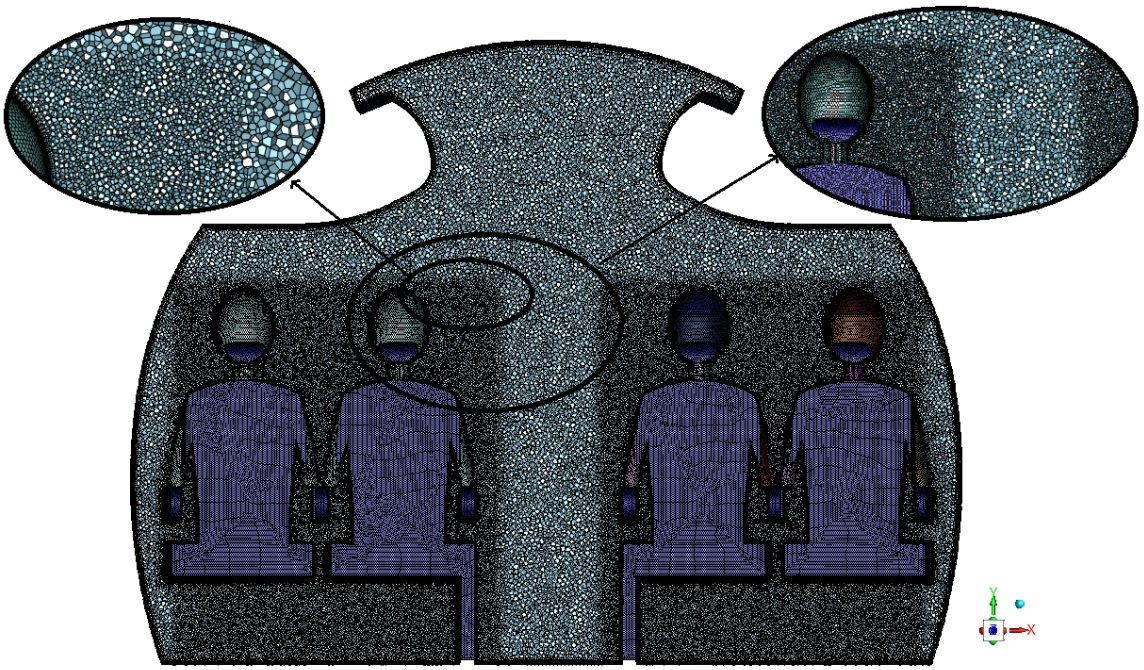

Figure 19: Polyhedral volume mesh with prism layers near walls and two BOI surrounding the passengers.

3.5.4 Solver setup

Steady state simulations are carried out in ANSYS Fluent 19.2, likewise "Case 0: Human in a 3D room". Pressure based solvers are chosen due to low velocity flows in the aircraft cabin. The RNG K-epsilon model with Enhanced wall treatment is employed for turbulence as it was shown to be favoured for indoor flow simulations. The solver setup can be deeply consulted in Abhishek et. al. [2], for the present thesis only two modifications are carried out. These modifications are: addition of radiation model and addition of buoyancy forces to the domain.

Discrete Ordinates is used to model radiation, and values for Theta and Phi Divisions are 3 and Theta and Phi pixels are 2. Increasing the discretization of Theta Divisions and Phi Divisions to a minimum of 3, will achieve more reliable results. A finer angular discretization can be specified to better resolve the influence of small geometric features or strong spatial variations in temperature. Boussinesq approximation is used to model buoyancy forces in the domain.

Table 8: Solver Settings

Equations	Discretisation
p-v scheme	Coupled
Turbulence Model	RNG K-epsilon with EWT
Gradient	Least squares cell based
Turbulence	1^{st} order upwind
Momentum & Energy	2^{nd} order upwind
Species	2^{nd} order upwind
Discrete Ordinates	2^{nd} order upwind

3.5.5 Boundary Conditions

A cabin inlet velocity of 0.26 m/s is used for this study based on 50% of the required airflow rate per passenger as stated by FAR regulations. 100% of the airflow rate was not studied since convergence was not obtained. To achieve the free outflow from the domain, a pressure outlet of 0 Pa is set. The cabin wall and seats are assumed as adiabatic, meanwhile the human skin temperature is imposed by whether a fixed temperature of 31°C or coupled with the HTRM.
The boundary conditions that model the heat transfer problem are listed in Table 9. The temperature of the skin is set by the thermoregulatory model when a coupled simulation is applied.

Table 9: Boundary conditions applied

Region	Boundary Conditions	DV	DV-coupled
Inlet	Velocity Inlet	0.26 m/s	0.26 m/s
Outlet	Pressure Outlet	0 Pa	0 Pa
Wall	Adiabatic Wall	-	-
Human	No Slip Wall	31°C	T_{sk} from Fiala
Periodic Zone	Periodic Interface	-	-
		Case 1	Case 2 & 3

Three different cases have been studied. Case 1 consists of an uncoupled simulation with Displacement Ventilation, 'DV', and a fixed temperature of 31°C for every human. Case 2 consists of a coupled simulation with the right window passenger coupled, 'DV-coupled'. Case 3 consists also of a coupled simulation with both the right aisle and window passengers coupled, 'DV-coupled'.

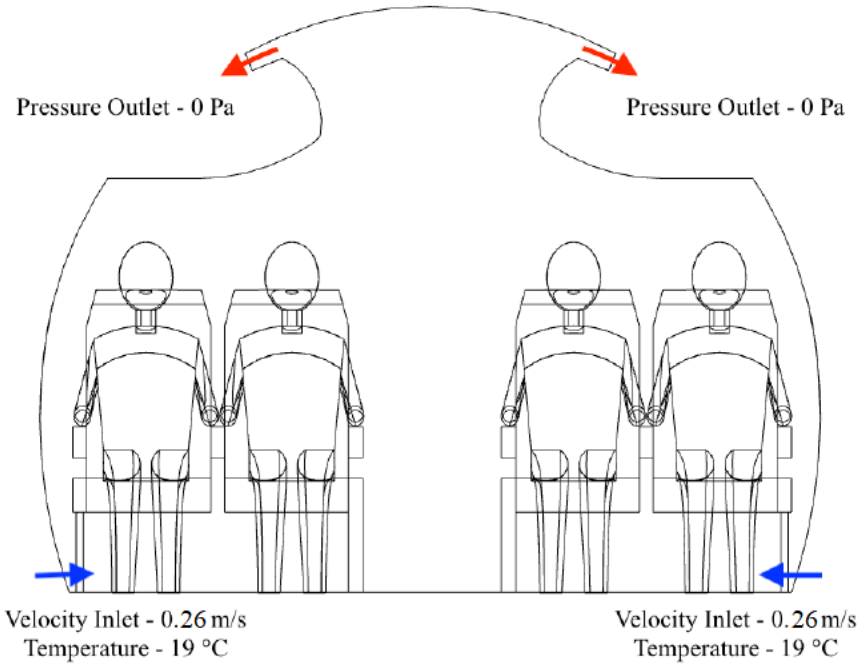

Figure 20: Illustration of boundary conditions used for Displacement ventilation type.

3.5.6 Thermal Comfort Study

The most commonly used thermal sensation-predicting model is the PMV model, developed in uniform and steady-state experimental conditions. It treats the body as a whole, in terms of physiological averages and sensations, and cannot predict transient responses. More advanced models developed in recent years can predict transient behavior, and also calculate physiological responses for multiple (six to twenty) body parts. However, they can only predict sensation at the whole-body level,and therefore have limited value for evaluating non-uniform environments. These are the case for example, of Zhang indices. All details of the model can be consulted in Zhang's articles (2010) [21] [22]. The comfort indices (both Zhang indices) were calculated by Matlab from the responses of the HTRM. The Zhang Local Sensation (SI) for each body part, is defined as a function of following parameters:

$$LocalSensation = f\left(T_{skin,i}, \frac{dT_{skin,i}}{dt}, \overline{T_{skin}}, \frac{dT_{core}}{dt}\right) \tag{14}$$

The Zhang Local Thermal Comfort (CI) for each body part, is defined as a function of following parameters:

$$LocalComfort = f\left(SI, S_0\right) \tag{15}$$

Where SI is the local sensation index for each body part and S_0 is the overall thermal sensation.

3.5.7 Calculation of Neutral skin temperature set points, $T_{sk_{set}}$

Using Zhang's method in the HTRM, the thermally neutral set point temperatures for each body part had to be recalibrated for HTRM by means of a simulation in a thermoneutral environment. A thermoneutral environment is not coherently defined in the literature. Thermoneutral temperature and humidity levels vary between sources, being 30°C and 50% RH (relative humidity of air) in Ferreira Yanagihara (2009), 30°C and 40% RH in Fiala (1999), 28.2°C and 30–32% RH in Smith (1991), or the values are not presented (Zhang 2003). For HTRM the operative temperature of 29°C and relative humidity of 45% were chosen as a thermoneutral environment. The set point temperatures were calculated without clothing and with the activity level of 1 Met. The thermally neutral set point temperatures of each body part by Zhang and HTM are presented in Table 10. With these set point temperatures the thermal sensation index was 0.05 (neutral) and the thermal comfort index was 1.47 (comfortable).

Table 10: Zhang's thermoneutral set point temperatures (Zhang 2003) and set point temperatures calibrated for HTRM for calculation of local thermal sensation

Body Part	Zhang's set point temperature °C	HTRM set point temperature, °C	Deviation, °C
Head	35,8	35,6	-0,2
Face	35,2	35,4	0,2
Neck	35,8	35,1	-0,7
Shoulder	34,2	34,2	0,0
Thorax	35,1	35,1	0,0
Abdomen	34,3	34,6	0,3
Arm	34,6	34,2	-0,4
Hand	34,4	35,3	0,9
Leg	34,3	34,6	0,3
Foot	33,3	33,3	0,0

4 Results

4.1 Velocity Distribution in the Cabin with Humans

Figure 21 displays the magnitude of velocity fields revealing that natural convection induced by humans is prevailing over forced convection from the inlet. Passengers connected to a HTRM display an "X-HTRM" mark. Symmetry in the flow is visible for the uncoupled case, Case 1, where the humans have all the same temperature. Case 2 breaks the symmetry of Case 1, due to the human coupled with HTRM that is a bit colder than the other ones, having an average skin temperature of 27.74°C. Case 3 is not as symmetric as Case 1, but humans (window and aisle) have a similar average skin temperature of 29.18°C and 29.16°C respectively.

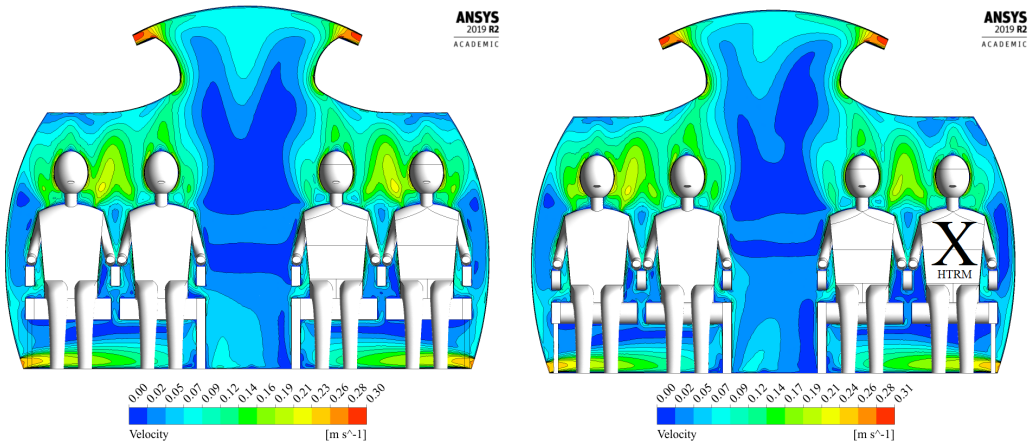

(a) Case 1. Uncoupled - $T_{sk} = 31°C$ **(b) Case 2. Coupled. 1 person -** $T_{sk} = Fiala$

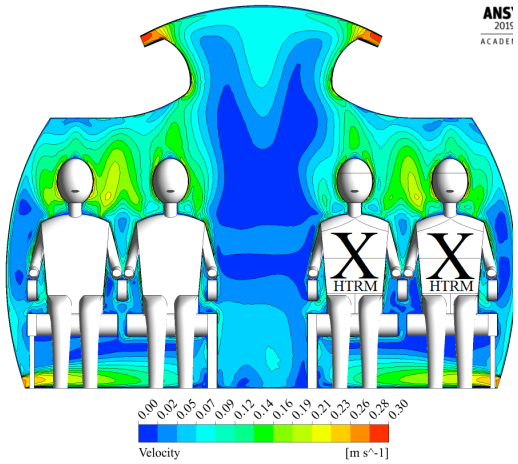

(c) Case 3. Coupled. 2 people - $T_{sk} = Fiala$

Figure 21: Velocity contour plots for different couplings

Figure 22 depicts the calculated airflow vector field for Case 3, the coupled simulation with 2 people connected to the HTRM. Case 1 and 2 were omitted because of having a really similar view. For all three cases, inlet mass flow runs parallel to the cabin floor until it reaches the aisle. Then it deflects upwards towards the seats zone, where the heat flow produced by the natural convection generated by the human beings is dominant.

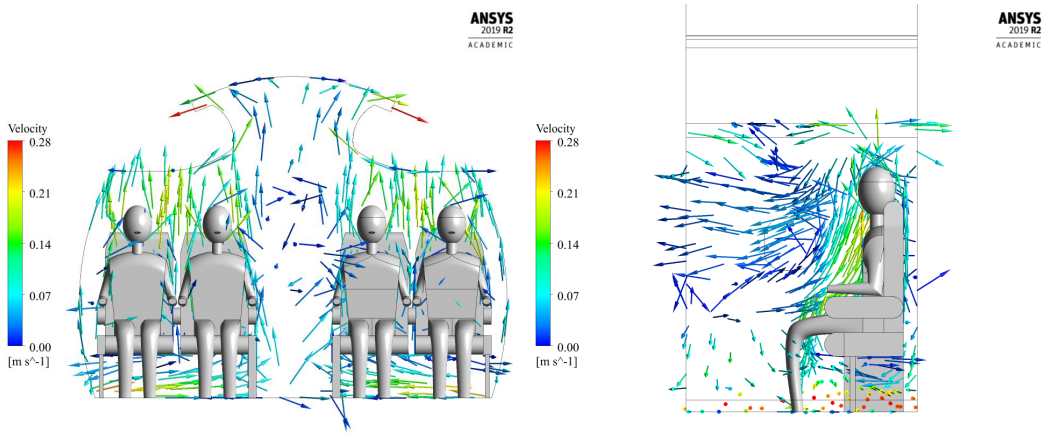

(a) Case 3. Coupled. 2 people (front view) **(b) Case 3. Coupled. 2 people (side view)**

Figure 22: Calculated airflow vector field for coupled simulation

4.2 Temperature Distribution in the Cabin with Humans

Temperature distribution contour plots in the cabin near the humans are depicted in Figure 23. The thermal plumes from the humans induce with the rising cool air from the inlets at the bottom and rises up towards the overhead bins. The temperature was more elevated above humans area while optimum (temperature range between 19°C to 27°C as required by FAR regulations) temperature was observed in the aisle and cabin.

For the coupled simulations (Figures 23b and 23c), the face is colder than the head due to heat losses through respiration. The right arm of the coupled person (Figure 23b) is significantly warmer than the left arm (28.8°C vs 27.7°C). That is because of the influence of the second human body next to it. Note that this example shows that the HTRM is sensitive to all nearby heat sources. Figure 23a shows that the two coupled humans have very similar skin temperatures.

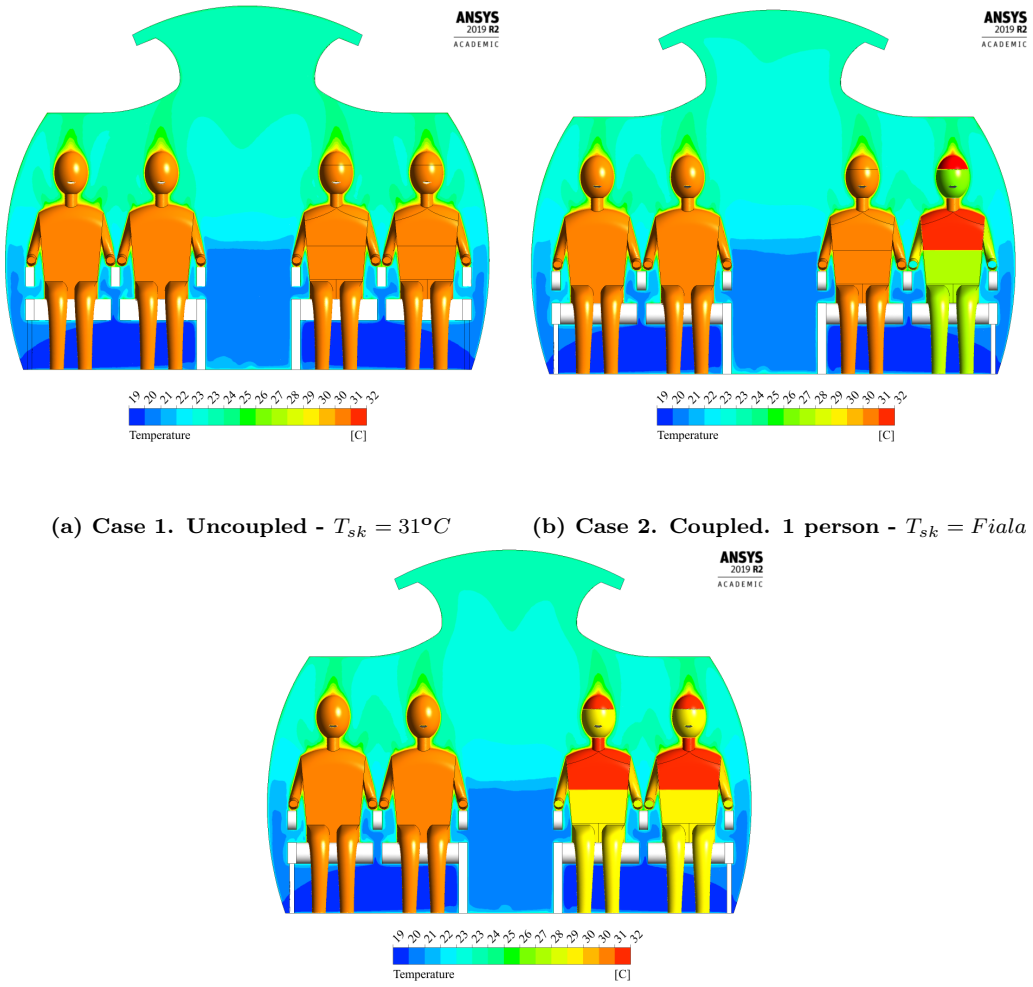

(a) Case 1. Uncoupled - $T_{sk} = 31^oC$ **(b) Case 2. Coupled. 1 person - $T_{sk} = Fiala$**

(c) Case 3. Coupled. 2 people - $T_{sk} = Fiala$

Figure 23: Temperature contour plots for different couplings

4.3 Heat Transfer Coefficient on Humans for different couplings

The surface heat transfer coefficient is the heat flux divided by the difference between the local wall temperature and the sorrounding air temperature. The heat transfer coefficient in all the three different coupling scenarios depicts the transfer of heat from the human to the cabin surrounding. The surface heat transfer coefficient is implemented as a User Defined Function in ANSYS Fluent, in order to have separately the radiative and the convective heat transfer coefficients. These parameters are iterated by means of heat fluxes until a balance is found between exchanges. Figure 24 show convective surface heat transfer coefficient (left side - Figures 24a,24c,24e) and radiative heat transfer coefficient (right side - Figures 24b, 24d, 24f) for the different couplings. For all of them, passengers experience a low heat transfer coefficient range overall, highest convective heat transfer coefficient is given on the lower legs, where the velocity is higher due to bottom located inlet diffusers. Figure 24a and 24b show symmetry in both radiative and convective heat transfer coefficients for the uncoupled case.

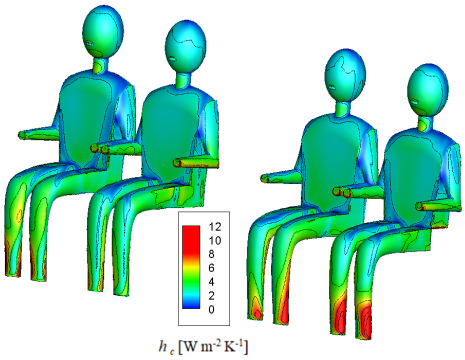

(a) Case 1. Uncoupled - $T_{sk} = 31^oC$

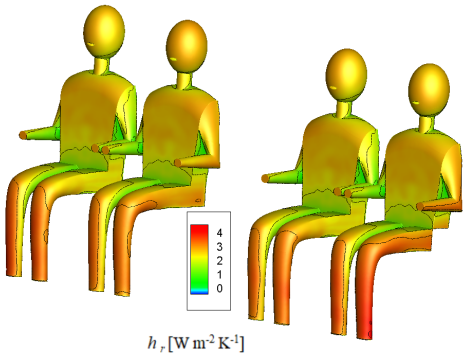

(b) Case 1. Uncoupled - $T_{sk} = 31^oC$

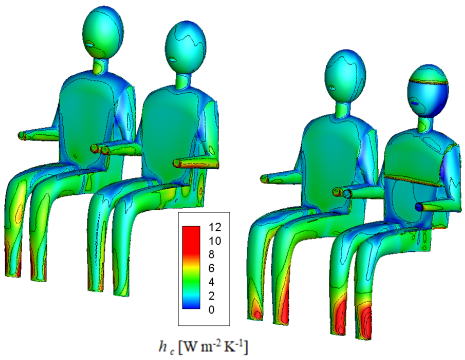

(c) Case 2. Coupled. 1 person - $T_{sk} = Fiala$

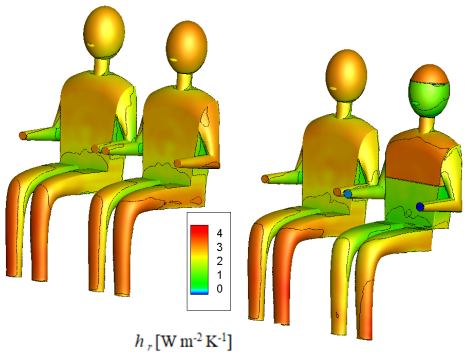

(d) Case 2. Coupled. 1 person - $T_{sk} = Fiala$

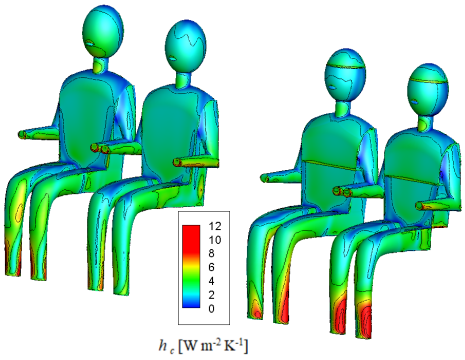

(e) Case 3. Coupled. 2 people - $T_{sk} = Fiala$

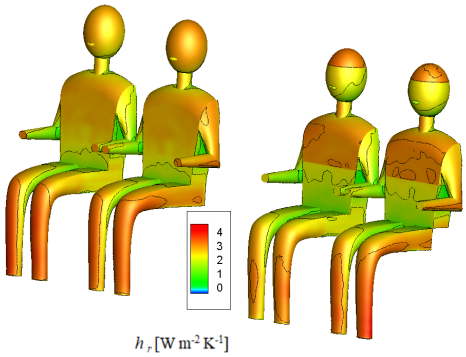

(f) Case 3. Coupled. 2 people - $T_{sk} = Fiala$

Figure 24: Convective (a, c & e) & Radiative (b, d & f) heat transfer coefficient for different couplings

4.4 Thermal Comfort Study

Figure 25 depicts both the Thermal Sensation Index (left) and the Thermal Comfort Index (right) for the three simulated cases. These results were obtained using Zhang's thermal comfort approach (2010) which has been explained in the Theory section and detailed in the Method section. From these Figures implemented in Matlab, an approach of both quantitative and qualitative comfort is displayed. 'LS - 1 Person WD' corresponds to the Local Sensation for the coupled simulation of only 1 person, which is sitting by the window. 'LS - 2 Person WD' corresponds to the coupled simulation of 2 people, and in this case the person analyzed is the person sitting by the window. 'LS - 2 Person AI' corresponds to the latter case but now the person sitting by the aisle is analyzed.

The resulting sensation scale ranges and comfort index ranges can be consulted in Tables 4 and 5 respectively.

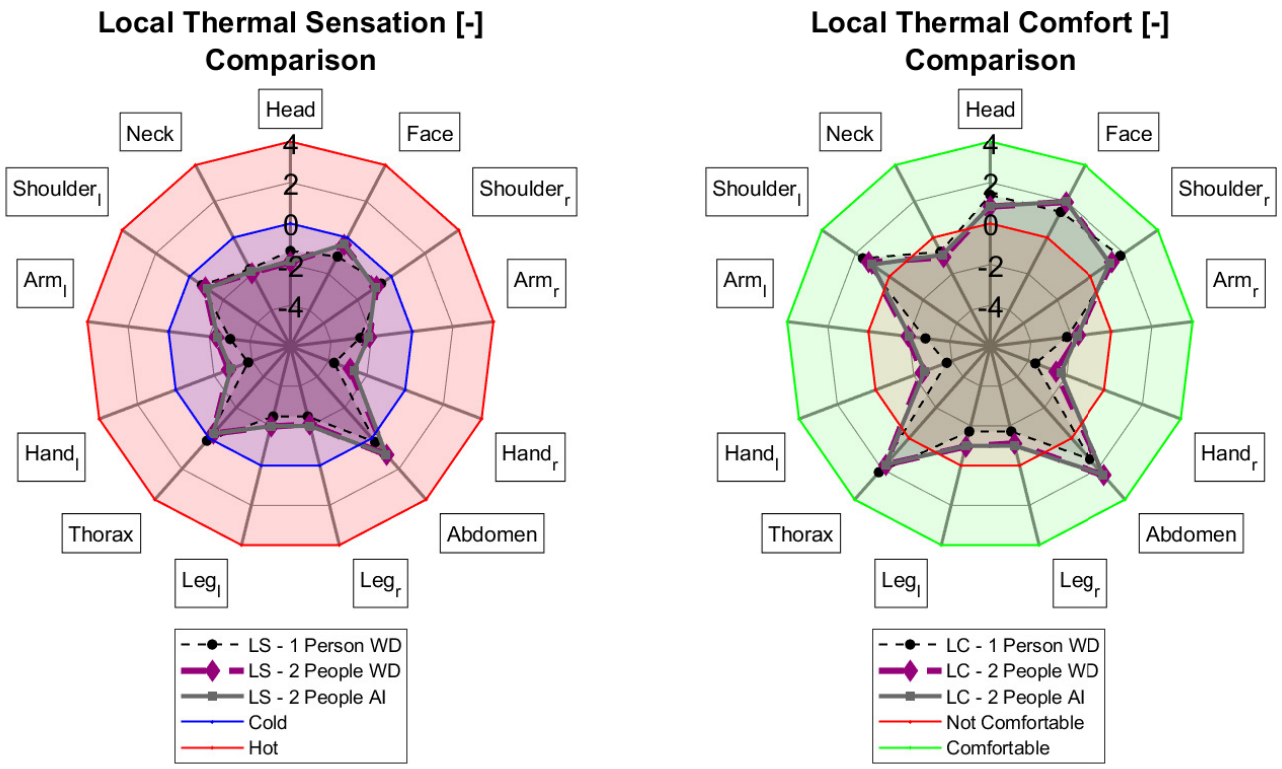

Figure 25: Predicted distribution of the Zhang Sensation and the Local Comfort indices on the passengers in a row of the cabin

Since the presented human is naked, and it is simulated in a cold environment (19°C of inlet air temperature), it is reasonable to appreciate a cold sensation for the overall body. The most affected parts are the extremities such as the arms, hands, legs and also the head. That is in logic with what is expected from the parts where heat transfer coefficient is greater (arms, hands and legs). The naked human was set to have a neutral reaction, that is, a 0 value in the thermal comfort scale when being in a environment whose average temperature was 29°C.

Thermal comfort follows a similar trend with thermal sensation. For most of parts, there were there is a neutral thermal sensation, there is a higher thermal comfort. Nonetheless, this is not exactly true for all parts, since for example, the head needs to be a bit cool to feel comfortable. Experimental regressions have been done by Zhang (2010) [21] for obtaining these different models and there is no specific linearity between them.

If comparing the three cases simulated, when simulating two people coupled ('LS - 2 People WD' & 'LS - 2 People AI'), they both have the same temperature skin fields. Then, it's reasonable that they both present almost coincident thermal sensation and comfort values. However, 'LS - 1 Person WD' shows to be a bit colder in the extremities as it was explained in the temperature distribution section.

Table 11: Overall thermal sensation and comfort comparison for humans in coupled simulations

Coupled sim.	1 Person WD	2 People WD	2 People AI
Overall Sensation	-1.62 Cool	-1.57 Cool	-1.59 Cool
Overall Comfort	-3.68 Very uncomfortable	-2.50 Uncomfortable	-2.43 Uncomfortable

Table 11 compares the overall thermal sensation and comfort for the two coupled cases. In the coupled simulation with two people (2 People WD & 2 People AI), it can be seen that the person sitting by the aisle feels slightly cooler than the person by the window. In the coupled simulated with one person (1 Person WD) the reason to feel very uncomfortable is due to the really uncomfortable feeling in the hands.

5 Discussion
Human in a 3D Room

5.1 Validation

Heat transfer coefficients comparison

5.1.1 Case 0. A) Uncoupled Case.

There are some differences in the methods of every author that lead to minor disagreements in the results. These are going to be explained thoroughly. The experimental manikin considered by De Dear [16] is wigged with shoulder-length hair, whereas the Computational manikin is bald for all CFD simulations (Sorensen) [17], (Cropper) [7]. For the head of the manikin, this probably explains the larger radiative heat transfer coefficient of the calculation compared to the measurements, as it can be seen in Figures 13b and 16b. This is also believed to explain the larger calculated value for the radiative heat transfer for the back of the manikin. It should be taken into account that no real humans were tested by neither De Dear, nor Sorensen nor Cropper, but all they used manikins.

Major differences for heat transfer coefficient are in the hands. This fact is due to the undevelopment of this body part, since hands are taken only as a slice of the end of the arm. If they were further developed, a good agreement may be achieved. Foot were not considered since the geometry didn't allow it.

Minor differences occur for the "head-face-neck" group, and this is because every author has separated the body in different body parts that don't really match. Sorensen and de Dear took the head in global as the head, face and neck. Meanwhile in this study, the head is only the section that would be protecting brain area. Face is also separated, as well as the neck. Sorensen and de Dear have a similar separation because they were using only a manikin model, regardless the inner body heat phenomena. Nevertheless, as soon as it is desired to couple a thermoregulatory model, the discretization of the body in CFD comes imposed by the number of parts that has the thermoregulatory model. That's why the present model is discretized similarly than Cropper, although with less body parts (13). Cropper had 59 body parts because a further developed Fiala model - IESDFiala - was used instead.

The same fact happens for the shoulders, Sorensen and de Dear called "shoulders" to the upper arm. It is translated into a higher value of convective heat transfer coefficient visible in the spider chart (see Figure 13a) for this part. For that, plots of the convective heat transfer coefficients on the body surface were plot intentionally to correct different parts spelling errors. Comparing Figures 15b and 15a, shoulders value match.

5.1.2 Case 0. A) Coupled Case.

Differences between the coupled simulation stay in the differences between Cropper and this study model, that basically is that Cropper is at standing position, meanwhile this study model is seating. It explains that this model achieves a lower radiative heat transfer coefficient (See Figure 16b). Since the flow is going from legs to head direction (going upwards), when the manikin is seated the legs make a "shadow" effect to the abdomen (see Figure 15) resulting in a decreasement of radiative heat transfer coefficient. This also has a decreasement in convective heat transfer coefficient, since the legs are blocking part of the flow that comes upwards. Moreover, Cropper results were given in 59 values of body parts that had to be matched to get a similar discretization to this study, which also introduces error.

Both, for the coupled and the uncoupled case, the heat transfer coefficients evaluated at whole body level agree satisfactorily with other CFD simulations and experimental data. An average value of 4.9 $[W \cdot m^2 \cdot K^{-1}]$ for radiant heat transfer coefficient and for convective heat transfer coefficient 3.1 $[W \cdot m^2 \cdot K^{-1}]$ are obtained. As it can be checked in the Tables 12 and 13 in the Appendix section.

Human in the Cabin

5.2 Methodology

The major new scientific knowledge of this thesis is combining the human thermal modelling with a thermal sensation and comfort model inside of a CFD simulation program. This approach enables i) calculating more realistically the interaction and non uniform transient heat transfer between the skin surface and the surrounding air and building structures and ii) taking into account the effect of human thermoregulation and individual human parameters on thermal sensation and comfort.

The coupled model presents inherent limitations which condition that it cannot be compared with experimental results such as photographs of the cabin taken by thermography. Naked humans are the reason for this fact, instead of having clothed ones. The shortage of time and being out of the scope of this thesis argue this reason. Subsequently, as soon as the cloth model is implemented in the HTRM, comparisons of temperature plots with experimental results will be available.

CFD model had to be run with 50% of the ventilation, not accomplishing FAR regulations, due to problems with convergence. It was taken as a measure to prioritize having the coupled model up and running. Probably the lack of convergence was due to a need for a higher mesh density in the aisle region (out of CPU capacity, being 13 million cells the maximum applicable). The mesh used was a replica from the mesh provided by Abishek and Raina [2] whose results proved to be mesh independent. Nonetheless, when applying Boussinesq model and activating subsequently natural convection, this mesh seemed to have trouble when modeling more chal-

lenging environments with higher ventilation. For every simulation, CPU time was intensive. Running the uncoupled simulation took 72h and the coupled simulations took around 5-6 days. 12 consecutive exchanges between Matlab and CFD were required till convergence was achieved. This fact also contributed to a higher difficulty if the mesh was wanted to be improved.

5.3 Thermal Comfort Study

The approach adopted for Thermal Comfort study, created by Zhang, presents an improvement over the PMV method. The commonly used Fanger's PMV method for thermal sensation and thermal comfort calculation takes into account the average operative temperature as a function of the indoor and average surface temperatures. It does not pay attention to the fact that the surface temperatures vary inside of a room, e.g. during the winter the heating devices are warmer and window surfaces colder than other surfaces. This uneven surface temperature distribution can cause thermal discomfort even though the average surface temperature might be acceptable.

Fanger's PMV method is a heat balance model, which views the human being as a passive recipient of thermal stimuli, assuming that the effects of the surrounding environment are explained only by the physics of heat and mass exchanges between the body and the environment, and neglecting the human thermoregulation system. The HTRM method takes into account the human tissue distribution and thermoregulation system in calculation of the skin and core temperatures, their change in time and the resulting local and overall thermal sensation and thermal comfort. Previous research has shown that Fanger's PMV method is valid for everyday prediction of the comfort vote only under severely restricted conditions, because it progressively overestimates the mean perceived warmth of warmer environments and the coolness of cooler environments.

Zhang's Method that was used in this thesis, has been successfully validated under various steady-state and transient indoor environment boundary conditions extracting the numerical regressions of the model from measurements made with real human beings.

5.4 Results

Displacement Ventilation was observed to be particularly causing human uncomfortabilities near inlet diffusers located at the bottom. Convective heat transfer coefficient was more elevated near the lower legs and also lower arms and a bit of the head for the latter reason. Adding to this the effect of also more elevated radiative heat transfer coefficient for the same parts due to surface to surface radiation, it caused a lower local skin temperature and consequently a colder thermal sensation. Expected cool sensations were obtained for a naked person due to being in a slightly cool environment (19^{o}C). Probably if a dressed manikin was tested, more comfortable sensations would be obtained.

5.5 Future work

For future work, some developments may be addressed in the scope of this thesis.

On the one hand, the HTRM could be further developed by adding different type of clothes. In this way, thermal comfort in different environments could be studied, such as which is the impact of cold/hot environments with several clothes. Validation should be taken into account, and there is the possibility to validate it with IESD-Fiala, easily accessible by the website created by Dr. Zhang ("http://www.jeplus.org/"). Hence, comparison with experimental thermography could be evaluated. After having this achieved, these clothes could be also modeled in the CAD of the human that is represented in the CFD model. The effect of simulating a naked human produces overestimating heat losses through convection and showing not real life results.

On the other hand, the CFD model could be tested with different ventilation types, such as mixed or personalized ventilation. The reader should keep in mind the complexity when modeling these challenging environments with strong whirls created by forced convection and also buoyancy effects dominating.

Moisture transfer could be also incorporated to the coupled simulation. If the cabin in CFD is decided to be wet, human sweating mass transfer can be incorporated into CFD as a source of moisture which modifies the relative humidity in the environment. Cropper [3] provides more details about how to do it.

Even though the current version of the Human Thermoregulatory Model, HTRM has some restrictions and the planned improvements will further develop the model, the current version has been shown in this thesis to estimate accurately enough the thermal sensation and thermal comfort of the human and the HTRM method is a major improvement to the currently used Fanger's PMV model.

A comparison study for a steady simulation could be carried out in order to appreciate the difference between a coupled simulation with several exchanges and a linear coupled simulation. A linear coupled simulation means that first the CFD case is converged with an initial set of skin temperatures and CFD output is directly passed to the HTRM. It would give directly a response of thermal comfort as it was the first iteration or the first exchange. Note that some errors will occur due to dismissing some of the effects of the interaction between the environment and the human body, but the study of this error may be of interest to save CPU time.

6 Conclusions

The main objective of this master thesis has been achieved. A coupled simulation technique has been developed that enables a multi-segmented model of human thermal comfort and physiology to exchange data with a commercial CFD program called Ansys Fluent. Initially it was developed for a 3DRoom and it was finally applied to the passengers of an Aircraft Cabin where Displacement ventilation was studied.

The presented numerical thermal comfort predictions are based on the solution of the Reynolds-averaged Navier-Stokes equation using the Boussinesq approximation and modeling of surface to surface thermal radiation in an aircraft cabin and a 3D room, and the coupling with the finite element code HTRM in Matlab. The latter allows to simulate the heat transport within the passengers and the perceived temperature and comfort of passengers. The way that the coupling algorithm has been programmed, makes possible that both steady and transient simulations can be studied. These transient effects will also be taken into account even for the thermal comfort study.

Comparisons of the predictions for 3D room by the coupled system with published experimental data and previous CFD studies show favourable agreement on the overall whole body mean heat transfer coefficients in still air conditions. The differences that can be observed in some body parts are suspected to be due, in part, differences in surface area between the computational manikin used in this study, and the experimental nude female manikin and posture. The comparisons described so far represent a relative simple case, in which the manikin is placed in an initially uniform environment. In the next step, Case 1: Human in an aircraft cabin, the responses of the coupled system to more challenging and non-uniform environments are investigated.

Regarding the aircraft cabin, the only objective that was not achieved was analyzing different ventilation systems, due to the high complexity for achieving convergence when running CFD cases such as mixing or personalized ventilation. In order to compensate this lack, a newly improved thermal comfort model was integrated in HTRM. The advantages over traditional traditional Fanger's PMV are, on the one hand the high range of environmental applications: non-uniform and transient environments are applicable, and also, having local and global parameters to study comfort for each of the body parts. It was shown that with the presented approach a qualitative and quantitative thermal comfort prediction is possible.

Thermal sensation and comfort results fit to the expected tendencies due to the simulated thermal environment. In the considered ventilation configuration, main drawbacks of thermal comfort for the passengers have been identified: draft risk at outward pointing the legs, arms and hands. The predicted discomfort due to draft risk at the hands and legs is furthermore intensified by a cold local thermal comfort.

References

[1] Espuna JC. Development of a Human Thermoregulatory Model for Aviation Related Application. 1st ed. LiU; 2019.

[2] Raina A, Venkatesan LS. CFD Study on Different Aircraft Cabin Ventilation Systems. 1st ed. LiU; 2020.

[3] Cropper PC, Yang T, Cook M, Fiala D, Yousaf R. Coupling a model of human thermoregulation with computational fluid dynamics for predicting human–environment interaction. 2010;Available from: `https://doi.org/10.1080/19401491003615669/`.

[4] Short CA, Shujian N, Weng W. Design guidance for naturally ventilated theatres. 2005;.

[5] Murakami S, Kato S, Zeng J. Combined simulation of airow, radiation and moisture transport for heat release from a human body. 1999;.

[6] Al-Mogbel A. A Coupled Model for Predicting Heat and Mass Transfer from a Human Body to its Surroundings. 2003;.

[7] Cropper PC, Yang T, Cook M, Fiala D. Exchange of simulation data be- tween CFD programmes and a multisegmented human thermal comfort model.;.

[8] Fiala D, Bunzl A, Lomas KJ, Cropper PC, Schlenz D. A New Simulation System for Predicting Human Thermal and Perceptual Responses in Vehicles. 2004;.

[9] Dixit A, Gade U. A case study on human bio-heat transfer and thermal comfort within CFD. 2015;.

[10] Inc A. ANSYS Fluent UDF Manual. ANSYS Inc.; 2013.

[11] Martinho N, Lopes A, da Silva MG. Evaluation of errors on the CFD computation of air flow and heat transfer around the human body. 2012;.

[12] Zhang Y, Yang T. Simulation of human thermal responses in a confined space. 2008;.

[13] Yang J, Cook MJ. Modelling heat transfer and physiological responses of unclothed human body in hot environment by coupling CFD simulation with thermal model. 2017;.

[14] Murakami S, Kato S, Zeng J. Flow and temperature fields around human body with various room air distributions: CFD study on computational thermal manikin—Part I. 1997;.

[15] Gao N, Niu J, Zhang H. CFD Study of the Thermal Environment around a Human Body: A Review. 2005;.

[16] de Dear R, Arens E, Oguro ZHM. Convective and radiative heat transfer coefficients for individual human body segments.;.

[17] Sorensen D, Voigt L. Modelling flow and heat transfer around a seated human body by computational fluid dynamics. 2002;.

[18] Treeck CV, Frish J, Pfaffinger M, Rank E, S Paule IS, Schwab R. Integrated thermal comfort analysis using a parametric manikin model fr interactive real-time simulation. 2009;.

[19] Fiala D. Dynamic Simulation of Human Heat Transfer and Thermal Comfort. PhD thesis. 1999;.

[20] Inc A. ANSYS Fluent Users Guide. ANSYS Inc.; 2013.

[21] Zhang H, Arens E, Huizenga C, Han T. Thermal sensation and comfort models for non-uniform and transient environments: Part I: Local sensation of individual body parts.;.

[22] Zhang H, Arens E, Huizenga C, Han T. Thermal sensation and comfort models for non-uniform and transient environments: Part I: Local comfrt of individual body parts.;.

[23] ANSYS I. ANSYS as a Server Example: MATLAB Setup. Release 2019 R1, January;.

[24] ANSYS I. ANSYS Fluent as a Server User's Guide. Release 15.0, November;.

[25] Tanabe S, Kobayashi K, Nakano J, Ozeki Y, Konishi M. Evaluation of thermal comfort using combined multi-node thermoregulation (65MN) and radiation models and computational fluid dynamics (CFD). 2002;.

[26] Gao N, Niu J, Zhang H. Coupling CFD and Human Bodt Thermoregulation Model for the Assessment of Personalized Ventilation . 2006;.

[27] Nielsen P, Murakami S, Kato S, Topp C. Benchmark tests for a computer simulated person. ISSN 1395-7953 R0307. 2003;.

A First appendix

A.1 Tables for convective heat transfer coefficient

Table 12: Radiative heat transfer coefficient for different segments of a seated human body. Units in $[W \cdot m^2 \cdot K^{-1}]$ (3D-Room Study)

	Body segments	Dear	Soren	Uncoupled	Cropper	Coupled
1	Head	3,9	5,2	5,6	5,4	5,7
2	Face	3,9	5,2	5,2	5,7	5,0
3	Neck	3,9	5,2	4,6	5,5	4,7
4	Shoulder_l	4,8	4,6	4,8	5,6	4,9
5	Shoulder_r	4,8	4,6	4,8	5,6	4,9
6	Thorax	4,6	4,7	5,3	4,4	5,4
7	Abdomen	4,6	5,1	4,5	5,2	4,3
8	Arm_l	5	4,3	4,4	4,3	4,3
9	Arm_r	5	4,3	4,4	4,2	4,3
10	Hand_l	3,9	4,1	5,4	4,2	5,3
11	Hand_r	3,9	4,1	5,4	3,8	5,3
12	Leg_l	5,4	5,1	4,8	5,0	4,8
13	Leg_r	5,4	5,1	4,8	5,1	4,7
	Whole body	4,5	4,8	4,9	4,8	4,9

Table 13: Convective heat transfer coefficient for different segments of a seated human body. Units in $[W \cdot m^2 \cdot K^{-1}]$ (3D-Room Study)

	Body segments	Dear	Soren	Uncoupled	Cropper	Coupled
1	Head	3,7	3,6	2,4	2,7	3,4
2	Face	3,7	3,6	4,3	3,3	3,4
3	Neck	3,7	3,6	3,6	1,7	3,1
4	Shoulder_l	3	2,7	1,8	1,4	1,3
5	Shoulder_r	3	2,7	1,9	1,3	1,3
6	Thorax	3	2,2	2,7	3,0	3,2
7	Abdomen	2,6	2,2	2,8	1,7	2,3
8	Arm_l	3,8	3,8	3,9	3,3	3,5
9	Arm_r	3,8	3,8	3,9	3,3	3,5
10	Hand_l	4,5	4,5	5,7	4,6	5,1
11	Hand_r	4,5	4,5	5,7	4,5	5,2
12	Leg_l	3,7	3,2	3,1	2,9	2,9
13	Leg_r	3,7	3,2	3,1	2,9	2,9
	Whole body	3,3	3,1	3,1	3,1	3,1

A.2 Manikin body part segmentation

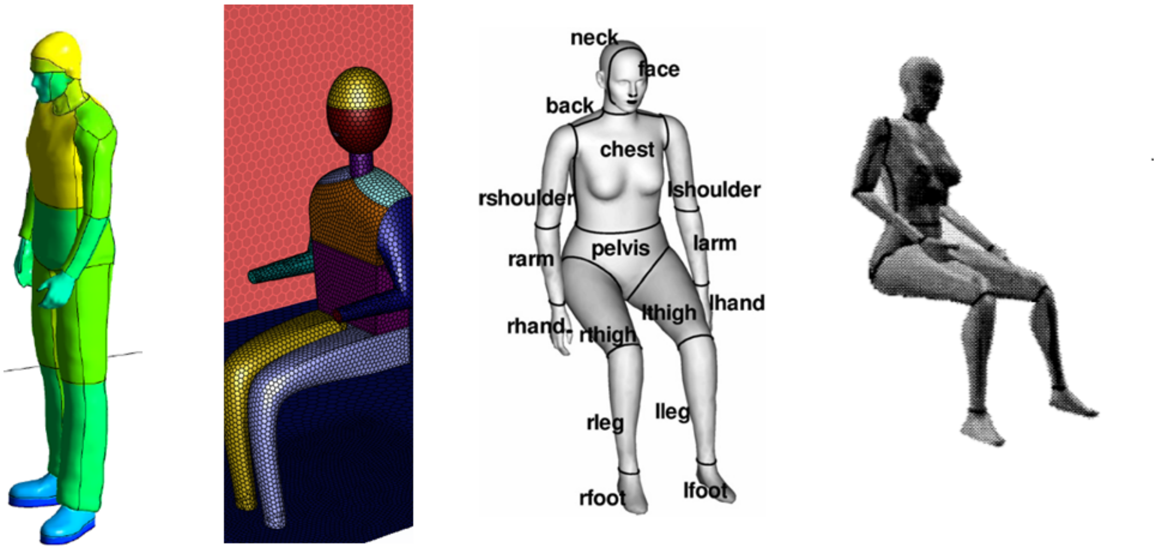

a) Cropper b) Bernat c) Sorensen d) de Dear (EXP)

Figure 26: Different human manikins with segmentation of body parts for each study considered to be compared in this report.

A.3 Code

In this section, two Matlab listings are included: the coupling script that controls the Matlab-CFD simulation and the function of Writing Output Parameters.

```
%%% WARNINGS THINGS TO DO:

%%% Cautions to run the PROGRAM: to have all Files together:
%%% 1) aas_Fluent Connections
%%% 2) 'HTRMFighter_function_onlyh.m'
%%% 3) FLUENT Directory \\ OR \\ Connect by code with FLUENT Directory

%%%% Launch Fluent in Standalone Mode. AAS = 1. (See Manual Fluent
    Users
%%%% as a Server Guide).
%
% Modified last time 06/06/2020 19:07
%
%%%%%%%%%%%%%%%%%%%%%%%%%%%%%%%%%%%%%%%%%%%%%%%%%%%%%%%%%%%%%%


%% Basic Connection %%%% RUN THIS SECTION   Once per session

orb=initialize_orb(); %initialize aaS
load_ansys_aas();
fluent=actfluentserver(orb,'aaS_FluentId.txt'); %connect to ANSYS
    products
```

```
tui=fluent.getSchemeControllerInstance();
tui.doMenuCommandToString('report summary')
%actwbserver('aaS_WbId.txt') %To connect Matlab with WorkBench

%tui.doMenuCommandToString('define operating conditions gravity yes 9.8
    0.0 0.0');

%% Read the case %%%%
%tui.doMenuCommand('file read case \"C:\myfolders\flntgz123604.cas\"')
tui.doMenuCommand('file read case \"//ad.liu.se/coop/i/IEI MVS Thesis/
    Marco and Eva/3DROOM/StandaloneFluent/Case&Data/FLTG 14 1rcoupled.
    cas.gz\"')
tui.doMenuCommand('file read data \"//ad.liu.se/coop/i/IEI MVS Thesis/
    Marco and Eva/3DROOM/StandaloneFluent/Case&Data/FLTG 14 1rcoupled.
    dat.gz\"')

%%%%%%%%%%%%%%%%%%%%%%%%%%%%%%%%%%%%%%%%%%%%%%%%%%%%%%%%%%%%%%%%%%%%%%%
% RUNNING COUPLING PROCESS %%

elements = 15; % Number of Body Part; %Feet excluded
elements_CFD = 13;
error = 1;
exchange = 0;

% %%Initialization of output variables:

    q_conv_CFD          = zeros(elements,1);
    q_tot_CFD           = zeros(elements,1);
    q_rad_CFD           = zeros(elements,1);
    h_conv_CFD          = zeros(elements,1);
    h_rad_CFD           = zeros(elements,1);



  input_T      = {'T_head', 'T_face', 'T_neck', 'T_shoulder_l',
           'T_shoulder_r',...
                  'T_thorax', 'T_abdomen', 'T_arm_l', 'T_arm_r', '
    T_hand_l', 'T_hand_r',...
                  'T_leg_l', 'T_leg_r', 'T_feet_l', 'T_feet_r'};

  output_q_tot          = {'q_tot_head', 'q_tot_face',
                     'q_tot_neck', 'q_tot_shoulder_l',
                'q_tot_shoulder_r',...
                           'q_tot_thorax','q_tot_abdomen', '
    q_tot_arm_l', 'q_tot_arm_r', 'q_tot_hand_l', 'q_tot_hand_r',...
                           'q_tot_leg_l', 'q_tot_leg_r', '
    q_tot_feet_l', 'q_tot_feet_r'};
  output_q_rad          = {'q_rad_head', 'q_rad_face',
                    'q_rad_neck', 'q_rad_shoulder_l', 'q_rad_shoulder_r
    ',...
                           'q_rad_thorax', 'q_rad_abdomen', '
    q_rad_arm_l', 'q_rad_arm_r', 'q_rad_hand_l', 'q_rad_hand_r',...
                           'q_rad_leg_l', 'q_rad_leg_r', '
    q_rad_feet_l', 'q_rad_feet_r'};


%% Run the HTRM for the first time and have an initial skin temperature
    (T_sk)
```

```
63
T_sk = HTRMFighter_function_onlyh_icl0(h_conv_CFD,h_rad_CFD); %T_sk_CFD
    = []; initially
65 [T_ref,~,~,~,~,~,~,~,~,~] = HTRMFighter_initialconditions(); %%[?C].
    Initial Sorrounding Air Temperature (%It is used to calculate h_conv
    ,h_rad)
T_wall = T_ref; %For Croppers example
67
%% DATA EXCHANGE CFD   MATLAB Loop
69 while error > 0.01

71     T_sk_old = T_sk; % Skin Temperature in the previous Exchange STEP.

73     T_sk_Kdegree = T_sk+273.15; % Fluent requires temperature in ?
    Kelvin

75 %% % SET INPUTParameters for CFD simulation
            %INPUTS: Skin Temperature, mass fraction,
77
for input_elem = 1:elements_CFD
79 tui.doMenuCommandToString(strjoin({'define parameters input parameters
    edit' ,strcat('\"',input_T{input_elem},'\"'),strcat('\"',input_T{
    input_elem},'\"'),num2str(T_sk_Kdegree(input_elem))}));
end
81
%% SOLVE SOME CFD ITERATIONS; maybe initialize is required before? (
    only first
83 %%time)
tui.doMenuCommand('solve iterate 10'); %SOME COMPOLSORY ITERATIONS TO
85 %ENSURE FLOW STABILIZATION AFTER CHANGING BOUNDARY CONDITIONS.


87
%% Stop the CFD calculations BEFORE Full Convergence IN order TO
    EXCHANGE
89
tui.doMenuCommand('solve monitors residual check convergence yes yes
    yes yes no no no no');
91          % Turns RESIDUAL STOP CRITERIA to be ON only: Momentum &
            % Continuity
93          %
            %
95          %   Check convergence of continuity residuals?[yes]
            %   Check convergence of x velocity residuals? [yes]
97          %   Check convergence of y velocity residuals? [yes]
            %   Check convergence of z velocity residuals? [yes]
99          %   Check convergence of energy residuals? [no]
            %   Check convergence of k residuals? [no]
101         %   Check convergence of epsilon residuals? [no]
            %   Check convergence of do intensity residuals? [no]
103         %%
tui.doMenuCommand('solve monitors residual convergence criteria 1e 03 1
    e 05 1e 05');
105 %%
tui.doMenuCommand('solve iterate 300'); %EXTRA Iterations to be STOPPED
107          ...BEFORE 300.

109 %% % %% REPORT
report = tui.doMenuCommandToString('report summary no');
```

```
111
%% EXAMPLE: GET Output Parameters from CFD simulation...
113
 %OUTPUTS: (q_conv, q_rad,)
115
 %%Notes. H calculated by Fluent directly is h_tot!!
117

119   %%  WRITE OUTPUT PARAMETERS
    tic
121 for output_elem = 1:elements_CFD

123 q_rad_CFD(output_elem)  = WriteOutputParameterByName(output_q_rad{
      output_elem});
    q_tot_CFD(output_elem)  = WriteOutputParameterByName(output_q_tot{
      output_elem});
125
    end
127 q_conv_CFD = q_tot_CFD    q_rad_CFD;

129 %%%%%%%%%%%%%%%%%%%%%%%%%%%%%%%%%%%%%%%%%%%%%%%%%%%%%%%%%%%%%%%%%%%%%%%%
    %      %%% COMPUTE h_conv, h_rad
131 for output_elem = 1:elements_CFD
    [h_conv_CFD(output_elem),h_rad_CFD(output_elem)] = heat_transfer_coeff(
      q_conv_CFD(output_elem),q_rad_CFD(output_elem),T_sk(output_elem),
      T_ref,T_wall);
133 end
    toc
135 %[h_conv_CFD(output_elem),h_rad_CFD(output_elem)] = heat_transfer_coeff
      (q_conv_CFD(output_elem),q_rad_CFD(output_elem),T_sk_CFD(output_elem
      ),T_ref,T_wall)

137 %%


139
    % COMPUTE FIALA T_skin (15), mass fraction (15). (for next EXCHANGE
      step)
141 T_sk = HTRMFighter_function_onlyh_icl0(h_conv_CFD,h_rad_CFD);

143 %%%%
    T_mean_sk = mean(T_sk);
145 T_mean_sk_old = mean(T_sk_old);

147 %%%% CONDITION TO END LOOP %%

149 %     error
    % % Cropper: "Loop is ended if: the difference in mean body surface
151 % % temperature between consecutive data exchanges is less than a pre
      set
    % % threshold. (By now, it is calculated with  T skin from Fiala,
      otherwise it would
153 % % be just required to change it for CFD coming T skin (it is the same
       for naked person)

155 error = abs(T_mean_sk    T_mean_sk_old);

157
```

```
% END OF THE EXCHANGE.
% T_sk_near T_sk is < x %. (That is the difference between skin of CFD and
% skin of HTRM. (with a WHILE in the BEGINNING)
%
exchange = exchange+1;
fprintf('Exchange Number has been completed   %d, with an error   %d', exchange,error');
end

%%%% EXCHANGE FINISHED %%%%

disp('Data exchange has been completed   Skin is converged');

%% Run the CFD calculations TO Full Convergence
                % After having skin temperature stabilized, flow nearby
                % might not have converged. Further CFD iterations may be
                % required.

tui.doMenuCommand('solve monitors residual check convergence yes yes yes yes yes yes'); % Turns RESIDUAL STOP CRITERIA to be ON only: ALL.
tui.doMenuCommand('solve monitors residual convergence criteria 1e-05 1e-05 1e-05 1e-05 1e-05 1e-05');

tui.doMenuCommand('solve iterate 3000'); %EXTRA Iterations to be STOPPED
...BEFORE 3000.

disp('CFD is converged');
```

Listing 1: Code of coupling simulation - CFD-Matlab.

```
function [output_value] = WriteOutputParameterByName(output_parameter)


% This function writes an Output parameter to Matlab that already exists in Fluent
%
%
%
% Inputs     >  Name of the parameter (in string)
%
% Outputs    >  Numerical value (in long)
%
% Modified last time 27/04/2020 12:35
%
%%%%%%%%%%%%%%%%%%%%%%%%%%%%%%%%%%%%%%%%%%%%%%%%

orb=initialize_orb(); %initialize aaS
%load_ansys_aas();
fluent=actfluentserver(orb,'aaS_FluentId.txt'); %connect to ANSYS products
tui=fluent.getSchemeControllerInstance();


```

```
one_param  = tui.doMenuCommandToString(strjoin({'define parameters
    output parameters  print to console' ,strcat('\"',output_parameter,'
    \"')})); %obtains_1parameter
23      charonepam = char(one_param);              % Turns into char the 1
    x1 automatically saved string into > 1x460 positions
      pos_start  = strfind(charonepam,'.') 1;    %To find the possition
    of the . which indicates the position of the OUTPUT NUMERICAL VALUE
25      pos_end    = strfind(charonepam,'e+')+3;  %To find the possition
    of the 'e+' which indicates the position of the OUTPUT NUMERICAL
    VALUE

27 output_value = str2num(charonepam(pos_start:pos_end)); %It extracts the
     value by cut positions.
```

Listing 2: Write output parameter function from Fluent to Matlab.

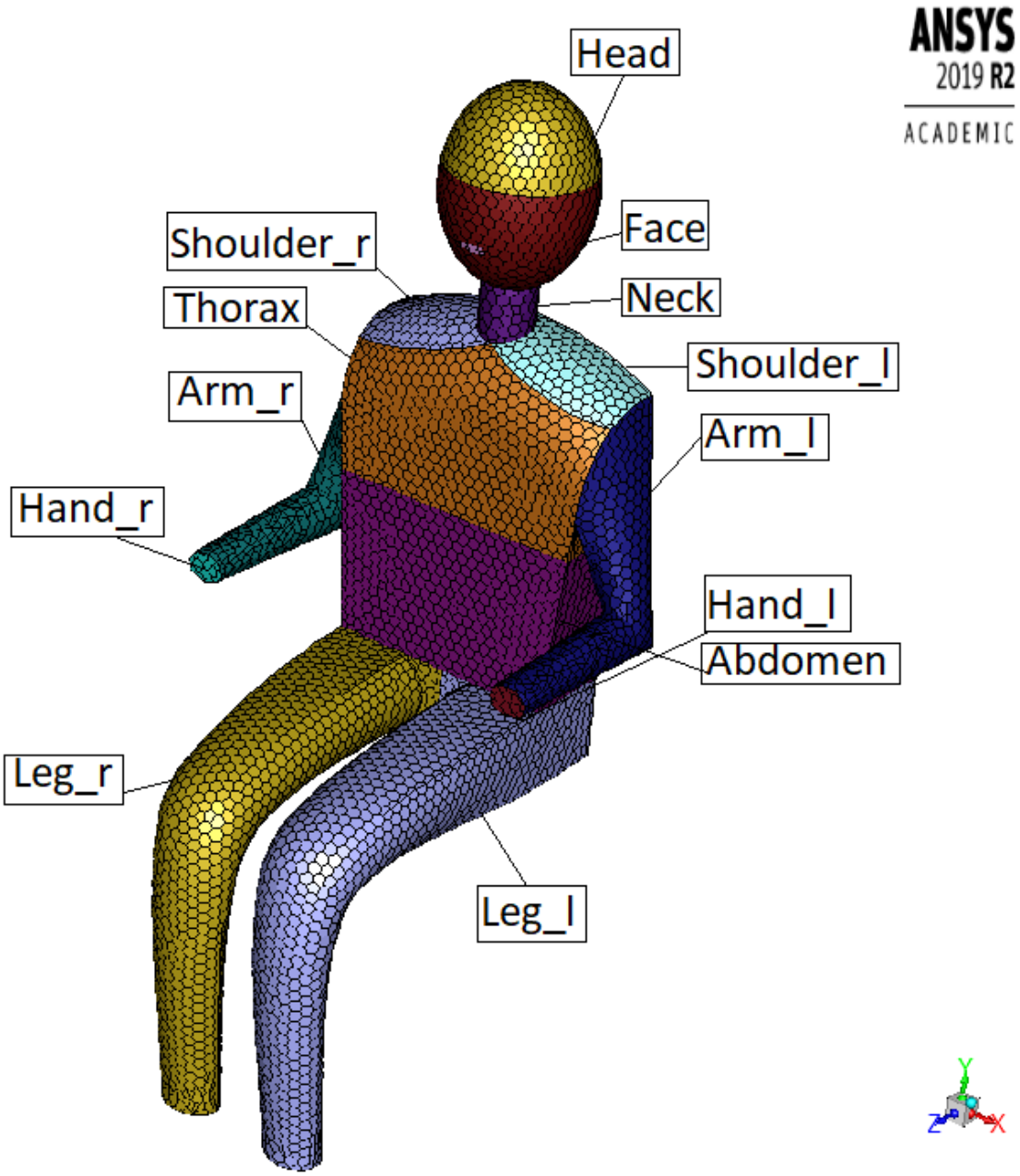

Figure 27: Segmentation of body parts for the study developed in this report.